A study on the role of phosphatidylserine in phospholipid flippase-mediated vesicle transport in yeast

A DISSERTATION

submitted to the Graduate School of Life Science,

Hokkaido University

in partial fulfillment of the requirements for the degree

DOCTOR OF LIFE SCIENCE

by

Miyoko Takeda

2014

Contents

Abstract

Phospholipid flippases translocate phospholipids from the exoplasmic to the cytoplasmic leaflet of cell membranes to generate and maintain phospholipid asymmetry. The genome of budding yeast encodes four heteromeric flippases (Drs2p, Dnf1p, Dnf2p, and Dnf3p), which associate with the Cdc50 family non-catalytic subunit, and one monomeric flippase Neo1p. Flippases have been implicated in the formation of transport vesicles, but the underlying mechanisms are largely unknown. Here I show that overexpression of the phosphatidylserine synthase gene *CHO1* suppresses defects in the endocytic recycling pathway in flippase mutants. This suppression seems to be mediated by increased cellular phosphatidylserine. Two models can be envisioned for the suppression mechanism. (1) Phosphatidylserine in the cytoplasmic leaflet recruits proteins for vesicle formation with its negative charge, and (2) phosphatidylserine flipping to the cytoplasmic leaflet induces membrane curvature that supports vesicle formation. In a mutant depleted for flippases, a phosphatidylserine probe GFP-Lact-C2 was still localized to endosomal membranes, suggesting that the mere presence of phosphatidylserine in the cytoplasmic leaflet is not enough for vesicle formation. The *CHO1* overexpression did not suppress the growth defect in a mutant depleted or mutated for all flippases, suggesting that the suppression was dependent on flippase-mediated phospholipid flipping. Endocytic recycling

was not blocked in a mutant lacking phosphatidylserine or depleted in phosphatidylethanolamine, suggesting that a specific phospholipid is not required for vesicle formation. These results suggest that flippase-dependent vesicle formation is mediated by phospholipid flipping, not by flipped phospholipids.

Abbreviations

ALPS motif, amphipathic lipid packing sensor motif; **CCVs**, clathrin-coated vesicles; **DAG**, diacylglycerol; **DIC**, differential interference contrast; **ER**, endoplasmic reticulum; **HPTLC**, high-performance thin-layer chromatography; **Lact-C2**, C2 domain of lactadherin **NBD**, 4-nitrobenzo-2-oxa-1,3-diazole; **P4-ATPases**, Type 4 P-type ATPases; **PC**, phosphatidylcholine; **PE**, phosphatidylethanolamine; PH, pleckstrin homology; **PI** phosphatidylinositol; **PS**, phosphatidylserine; SC, synthetic complete; SD, synthetic defined media; **TGN**, *trans*-Golgi network; **t-SNARE**, target soluble NSF-attachment protein receptor; **v-SNARE**, vesicle soluble NSF-attachment protein receptor; YPDA, yeast peptone dextrose adenine

Introduction

Type 4 P-type ATPases (P4-ATPases), highly conserved membrane proteins among eukaryotic cells, are phospholipid flippases that selectively transport phosphatidylserine (PS) and phosphatidylethanolamine (PE) from the exoplasmic to the cytoplasmic leaflet of the plasma membrane and internal membranes to generate and maintain asymmetrical distribution of phospholipids (1-4). P4-ATPase deficiencies are associated with human diseases (e.g. intrahepatic cholestasis type 1) (5). However, much remains to be learned about the functions and physiological and pathological importance of P4-ATPases.

In the budding yeast *Saccharomyces cerevisiae*, there are five P4-ATPases, Drs2p, Dnf1p, Dnf2p, Dnf3p, and Neo1p (**Fig.1**). Of these, Drs2p, Dnf1p and Dnf2p, and Dnf3p form a complex with Cdc50 family non-catalytic subunits, Cdc50p, Lem3p, and Crf1p, respectively, for their exit out of the endoplasmic reticulum (ER) and proper localization (6, 7). These four flippases are collectively essential for viability and have redundant roles for vesicle transport in various transport pathways (8, 9), including the early endosome-*trans*-Golgi network (TGN) retrieval pathway or the endocytic recycling pathway (7). Neo1p does not associate with Cdc50 family members, and thus might function without a non-catalytic subunit. Neo1p is an essential protein by itself, possibly because it is involved in various cell functions other than the endocytic recycling pathway,

including retrograde transport from Golgi to the ER (10) and membrane trafficking within endosomal/Golgi system (11).

Amino phospholipids PS and PE seem to be preferred substrates of flippases. *In vitro* studies using a fluorescent analog (4-nitrobenzo-2-oxa-1,3-diazole [NBD]-PS and NBD-PE) suggested that Cdc50p-Drs2p prefers PS with a minor activity toward PE (12-14). In contrast, Lem3p-Dnf1p and -Dnf2p translocate NBD-PE and NBD-phosphatidylcoline (PC) when they are localized at the plasma membrane (9, 15). However, since all these studies essentially employed a phospholipid analog or a lipid-binding peptide, it needs to be further demonstrated that phospholipids are involved in flippase functions *in vivo*.

Cdc50p-Drs2p, which is mainly localized to early endosome/TGN membranes, is implicated in the formation of clathrin-coated vesicles (CCVs) from these membranes (16-19). Because clathrin has no intrinsic lipid-binding ability, it is linked to membranes by adaptors, which bind to lipids and/or the cytoplasmic domains of cargo proteins (20). The AP-1 clathrin adaptor has been suggested to function downstream of Cdc50p-Drs2p (18, 19), but the underlying mechanisms are unknown.

One important question is how flippase activity is harnessed to form a transport vesicle. Flippases would influence physicochemical properties of

membranes by an asymmetric membrane structure with a high concentration of substrate lipids, such as PS and PE, in the cytoplasmic leaflet. These phospholipids could recruit adaptor proteins for vesicle formation by their specific properties (e.g. a negative charge of PS). A second important consequence of a flippase activity is an increase in phospholipid number within the cytoplasmic leaflet relative to the luminal leaflet. This could induce bending in the membrane toward the cytosol, a process that is essential to vesicle budding (21).

Here I show that overexpression of the PS synthase gene *CHO1*, which resulted in PS increase, suppressed defects in endocytic recycling of flippase mutants. My results suggest that PS in the cytoplasmic leaflet is not sufficient for vesicle formation and that flippase-mediated phospholipid translocation is coupled with vesicle formation.

Materials and Methods

Media and Genetic Methods

Unless otherwise specified, strains were grown in YPDA rich medium (1% Bacto yeast extract [Difco Laboratories, Detroit, MI], 2% Bacto-peptone [Difco], 2% glucose, and 0.01% adenine). Strains carrying plasmids were selected in synthetic medium (SD) containing the required nutritional supplements (22). Synthetic complete medium (SC) was SD medium containing all required nutritional supplements. When appropriate, 0.5% casamino acids were added to SD medium without uracil (SDA-U). For induction of the *GAL1* promoter, 3% galactose and 0.2% sucrose were used as carbon sources (YPGA, SG-U, and SGA-U) instead of glucose.(YPDA, SD-U, and SDA-U). When required, 2 mM ethanolamine and 2 mM choline were supplemented to medium to support growth of the *cho1*Δ and *psd1*Δ *psd2*Δ mutants, respectively. Standard genetic manipulations of yeast were performed as described previously (23). The lithium acetate method was used for introduction of plasmids into yeast cells (24, 25).

Escherichia coli strains DH5α and XL1-Blue were used for construction and amplification of plasmids.

Strains and Plasmids

Yeast strains constructed in the YEF473 background (26) are listed in **Table 1**.

Because flippase and *cho1*Δ mutants exhibit defects in tryptophan uptake (27), a strain in which *trp1*Δ*-63* was replaced with *TRP1* was constructed (YKT1066), and most strains used in this study were derived from this strain. PCR-based procedures were used to construct gene deletions and gene fusions with the *GAL1* promoter, GFP, and mRFP (26). Some gene deletions (*psd1*Δ and *psd2*Δ) were constructed by transformation with PCR-products from knockout strains. The *psd1*Δ *psd2*Δ mutant was a kind gift of Dr. S. Moye-Rowley (The University of Iowa). All constructs produced by the PCR-based procedure were verified by colony-PCR amplification to confirm the replacement occurred at the expected locus. When required, selection markers of mutant alleles were changed appropriately by cassette exchange (28).

The GFP-tagged Lact-C2 plasmid (pRS416-GFP-Lact-C2) (29) was purchased from Haematologic Technologies, Inc. (Essex Junction, VT). The *URA3::GFP-Lact-C2* strain was constructed by integrating the linearized pRS306-GFP-Lact-C2 into the *URA3* locus, and the *URA3::GFP-Lact-C2AAA* (Lact-C2-W26A, W33A, F34A) strain was similarly constructed. *Lact-C2AAA* (29), *CHO1(D148A)*, and *CHO1(D152A)* mutations were constructed by site-directed mutagenesis as described (30). The *LEU2::mRFP-SNC1* strain was constructed by integrating the linearized pRS305-mRFP-SNC1 into the *LEU2* locus, and the *LEU2::mRFP-SNC1(pm)* strain was similarly constructed. The

neo1-101::LEU2 strain was constructed by integrating the linearized pRS305-neo1-101-C, which contained only the carboxyl-terminal *neo1-101* mutation site fragment, into the *NEO1* locus. The plasmids used in this study are listed in **Table 2**. Schemes detailing the construction of plasmids and DNA sequences of nucleotide primers are available upon request.

Determination of the *neo1-101* Mutation Site

The *neo1-101* mutant gene was cloned by the gap repair method (31). The pRS316-NEO1ΔBglII plasmid was linearized with *Hind*III and *Hpa*I, followed by transformation into the *neo1-101* strain (YKT1651). Plasmids were recovered from several independent Ura^+ transformants and sequenced. One mutation, which changed GTG (Val) of the codon 1145 to ATG (Met) in the C-terminal cytosolic region of Neo1p, was identified.

Isolation of Multicopy Suppressors of the P_{GAL1}-*CDC50 neo1-101* Mutant

The P_{GAL1}-*CDC50 neo1-101* strain was transformed with a yeast genomic DNA library constructed in the multicopy plasmid YEp24 (32). Transformants were selected on SGA-U plate at 30°C and then replica-plated onto YPDA plates. Plasmids were recovered from the transformants that grew on YPDA, and those containing *CDC50* or *NEO1* were identified by PCR and eliminated. Restriction

enzyme digestion of the remaining plasmids indicated that twenty different clones were isolated. Nine of these plasmids reproducibly conferred growth on YPDA. Three clones that exhibited clearer suppression were chosen, and the genes responsible for the suppression were determined to be *CHO1*, *YCK1*, and *ART5* by fragment subcloning and DNA sequencing.

Microscopic Observations

Cells were observed using a Nikon ECLIPSE E800 microscope (Nikon Instec, Tokyo, Japan) equipped with an HB-10103AF super high-pressure mercury lamp and a 1.4 numerical aperture 100× Plan Apo oil immersion objective lens with appropriate fluorescence filter sets or differential interference contrast optics. Images were acquired using a digital cooled charge-coupled device camera (C4742-95-12NR; Hamamatsu Photonics, Hamamatsu, Japan) using AQUACOSMOS software (Hamamatsu Photonics). Observations are compiled from the examination of at least 100 cells. To visualize GFP- or mRFP-tagged proteins, cells were grown to early to mid-logarithmic phase, harvested, and resuspended in SDA- or SD-based medium. Cells were mounted on microslide glass and immediately observed using a GFP bandpass or G-2A (for mRFP) filter set.

Phospholipid Analysis

Cells were grown in 12 ml of appropriate medium containing 1 µCi/ml of [^{32}P]-orthophosphoric acid (Perkin Elmer-Cetus, Norwalk) to an OD_{600} of 0.5 for 12 h at 30°C to achieve steady state labeling. The cells were harvested by centrifugation, washed with sterile water, and transferred to screw-capped glass tubes. The cells were treated with 5% trichloroacetic acid for 1 h on ice and then washed with cold water three times. Phospholipids were extracted basically by the Bligh and Dyer method (33), using 0.1N HCl as the aqueous phase as described (34). The cells were resuspended in 1.2 ml of $CHCl_3$:MeOH:0.1 N HCl (1:2:0.8) and lysed by vortexing with glass beads for 3 min. 0.4 ml each of $CHCl_3$ and HCl/NaCl (0.1 N/ 0.5 M) was added, followed by centrifugation, isolation of the lipid-containing phase, and evaporation of the solvent. The extracted lipids were dissolved in appropriate volume of $CHCl_3$:MeOH (2:1) and analyzed by one-dimensional high-performance thin-layer chromatography (HPTLC) as described (35). The HPTLC plate (Merck, Darmstadt, Germany) was exposed to an imaging plate for 2 days, and the signal was detected and quantitated by using an FLA 3000 fluorescent image analyzer (Fuji Film, Tokyo, Japan). Phospholipids were identified by comparison with commercial standards (Avanti Polar Lipids, Alabaster, AL).

Results

Combination of *neo1-101* and *cdc50*Δ mutations results in synthetic defects in endocytic recycling

An allele of *NEO1*, *neo1-101* was obtained by previous screening for mutations that were synthetically lethal with *cdc50*Δ (36). Neo1-101p had a valine 1145 to methionine substitution in the C-terminal cytoplasmic region. *NEO1* is an essential gene, but the *neo1-101* mutation did not affect the growth rate (**Fig. 2A**). The *neo1-101* mutation was combined with conditional alleles of flippase genes, P_{GAL1}-*CDC50* and P_{GAL1}-*DRS2* alleles, whose expression is repressed by glucose. Both Cdc50p- and Drs2p-depleted *neo1-101* cells exhibited severe growth defects (**Fig. 2A**). The *neo1-101* mutation did not exhibit synthetic growth defects with *lem3*Δ or *dnf1*Δ *dnf2*Δ mutations (data not shown).

Because a previous study showed that Cdc50p-Drs2p, Lem3p-Dnf1/2p, and Crf1p-Dnf3p had redundant roles in the early-endosome to TGN recycling pathway (7), I examined whether the *neo1-101* mutation aggravated the recycling defect in Cdc50p-depleted cells. Dnf2p, which is mainly localized to polarized growth sites of the plasma membrane (8, 9, 36), is recycled from the plasma membrane *via* the early endosome to the TGN (37). The *neo1-101* mutant cells exhibited normal polarized localization of Dnf2p-GFP at a bud or a cytokinesis site (99%, n=143 budded cells) like wild type cells (99%, n=145)

(**Fig. 2B**). In the Cdc50p-depleted cells in which Cdc50p was partially depleted for 12 h in the presence of glucose, Dnf2p-GFP was internally accumulated in some cells, but most of the cells still exhibited polarized Dnf2p-GFP (90%, n=122) as reported previously for GFP-Snc1p (18). In contrast, in the Cdc50p-depleted *neo1-101* mutant, only 8% (n=127) of the cells exhibited polarized Dnf2p-GFP, and the remaining 92% accumulated Dnf2p-GFP in internal structures that seemed to be early endosome-derived abnormal membranes.

To confirm these results, I examined other cargos transported through this pathway. A vesicle soluble NSF-attachment protein receptor (v-SNARE) Snc1p, involved in the fusion of Golgi-derived secretory vesicles with the plasma membrane, is recycled through the endocytic recycling pathway (38). Tlg1p, an essential target soluble NSF-attachment protein receptor (t-SNARE) mediating fusion of endosome-derived vesicles with the TGN, is recycled between the early endosome and the TGN (39, 40). In wild-type cells, mRFP-Snc1p was localized to polarized plasma membrane sites like Dnf2p-GFP, whereas GFP-Tlg1p was observed as internal punctate structures reminiscent of endosomal/TGN membranes (**Fig. 2C**). In the Cdc50p-depleted *neo1-101* mutant, both mRFP-Snc1p and GFP-Tlg1p were localized to internal enlarged compartments (82%, n=124). These compartments were independent of a

TGN-marker Sec7p-mRFP (**Fig. 2D**), suggesting that they were early endosome-derived membranes. These results suggest that combination of *cdc50* and *neo1-101* mutations caused the synthetic defect in the retrieval pathway from the early endosome to the TGN.

Overexpression of the PS synthase gene *CHO1* suppresses the endocytic recycling defects in the Cdc50p-depleted *neo1-101* mutant

To obtain a clue to flippase functions, I isolated multicopy suppressors of the synthetic growth defect of the Cdc50p-depleted *neo1-101* mutant. *CHO1*, encoding the unique phosphatidylserine synthase in yeast, was isolated (**Fig. 3A**). Cho1p catalyzes the synthesis of PS from CDP-diacylglycerol (DAG) and serine in the ER (41). To confirm that the overexpressed Cho1p was normally localized to the ER membrane, I constructed the *CHO1-GFP* allele. *CHO1-GFP* was functional, because it complemented the choline auxotrophy and the cold-sensitive growth of the *cho1*Δ mutant (data not shown). The Cho1p-GFP overexpressed from a multicopy plasmid was colocalized with an ER marker Sec63p-mRFP (42) in the Cdc50p-depleted *neo1-101* mutant as well as in the wild type (**Fig. 3B**), indicating that the overexpressed Cho1p-GFP was normally localized to the ER. I confirmed that Cho1p-GFP was overexpressed in these strains, because the Cho1p-GFP signal was undetectable under the same condition

in a strain expressing Cho1p-GFP from its genomic locus (data not shown). The overexpressed *CHO1-GFP*, however, did not suppress the growth defect of the Cdc50p-depleted *neo1-101* mutant (data not shown), suggesting that Cho1p-GFP is somewhat less functional than Cho1p.

I examined whether the *CHO1* overexpression also suppressed the recycling defect of Dnf2p-GFP in the Cdc50p-depleted *neo1-101* mutant. When Cdc50p in the *neo1-101* mutant was depleted for 12 h in the glucose-containing synthetic medium (SDA-U), Dnf2p-GFP was polarized in 13% (n=142 budded cells) of the cells, which was slightly higher compared to the cells grown in YPDA rich medium (8%, Fig. 2B). The *CHO1* overexpression increased the cells with polarized Dnf2p-GFP to 36% (n=140) (**Fig. 3C**). This partial suppression was consistent with the partial suppression of the growth defect. Because it was previously shown that *CHO1* overexpression increased cellular PS levels (43), these results suggest that the endocytic recycling of Dnf2p-GFP was restored by increased PS.

To confirm that PS content was increased in the Cdc50p-depleted *neo1-101* mutant by *CHO1* overexpression, I analyzed phospholipid composition in the cells grown under the same condition as in Fig. 3C. Interestingly, I noticed that PS content was decreased from 17.0 ± 0.9% of the wild type to 11.1 ± 1.9% in the Cdc50p-depleted *neo1-101* mutant, whereas PI content was increased from

16.2 ± 2.4% to 22.4 ± 0.7% (**Fig. 3D**). The molecular basis for these phospholipid changes is currently unclear, but this seems to be specific to the Cdc50p-depleted *neo1-101* mutant, because these changes were subtle (PS) or not observed (PI) in the Cdc50p-depleted *dnf1*Δ *crf1*Δ mutant (**Fig. 4E**). Overexpressed *CHO1* resulted in 1.7-fold increase of PS content (from 11.1 ± 1.9% to 18.6 ± 0.6%) in the Cdc50p-depleted *neo1-101* mutant (**Fig. 3D**). In contrast, the phosphatidylinositol (PI) level was decreased from 22.4 ± 0.7% to 14.9 ± 0.8% by *CHO1* overexpression, probably because CDP-DAG is also a precursor for PI synthesis (44). Because the suppression was dependent on a remaining flippase (see below), increase of PS, a known substrate of flippases, seems to be responsible for the suppression.

To confirm that the suppression is dependent on the enzymatic activity of Cho1p, I examined the catalytically inactive mutants of Cho1p. The CDP-alcohol phosphotransferase motif was previously suggested as a catalytic site of the enzymes including Cho1p that catalyze the synthesis of a phospholipid by the displacement of CMP from a CDP-alcohol by a second alcohol to form a phosphoester bond. Two aspartic acid residues in this motif, Asp131 and Asp135, were shown to be essential for the catalytic activity of yeast cholinephosphotransferase (Cpt1p) (45). The corresponding residues in Cho1p, Asp148 and Asp152, were replaced with alanine to form Cho1p(D148A) and

Cho1p(D152A), respectively. As expected, neither *cho1(D148A)* nor *cho1(D152A)* complemented the choline auxotrophy and the cold-sensitive growth of the *cho1*Δ mutant (data not shown). As shown in **Fig. 3E**, overexpression of these *cho1* mutant genes did not suppress the growth defect of the Cdc50p-depleted *neo1-101* mutant. I confirmed that both the overexpressed Cho1p(D148A)-GFP and Cho1p(D152A)-GFP were normally localized to the ER as Cho1p-GFP was (data not shown).

The *CHO1* overexpression also suppresses the endocytic recycling defects in the Cdc50p-depleted *dnf1*Δ *crf1*Δ mutant

To examine whether the suppression was specific to *neo1-101*, I overexpressed *CHO1* in the Cdc50p-depleted *dnf1*Δ *crf1*Δ mutant in which Dnf2p-GFP could be also used as a marker for endocytic recycling. As shown in **Fig. 4A**, the *CHO1* overexpression suppressed the growth defect in the Cdc50p-depleted *dnf1*Δ *crf1*Δ mutant. In this mutant in which Cdc50p was depleted for 12 h, Dnf2p-GFP was accumulated in intracellular membranes, whereas mRFP-Snc1p(pm), a mutant of Snc1p, was localized to the plasma membrane (**Fig. 4B**). mRFP-Snc1p(pm) is normally transported to the plasma membrane by the exocytosis pathway, but is not endocytosed due to its defects in endocytosis (38). Thus, these results suggest that the Cdc50p-depleted *dnf1*Δ

*crf1*Δ mutant is defective in the endocytic recycling pathway, but not in the exocytosis pathway, and that Dnf2p-GFP was accumulated in early endosome-derived membranes. In the Cdc50p-depleted *dnf1*Δ *crf1*Δ cells, Dnf2p-GFP was localized to the plasma membrane only in 9% of the cells (n=107 budded cells), whereas it increased to 59% when *CHO1* was overexpressed (n=137) (**Fig. 4C**). These results suggest that the *CHO1* overexpression partially restored endocytic recycling of Dnf2p-GFP in the Cdc50p-depleted *dnf1*Δ *crf1*Δ mutant.

I also examined whether the *CHO1* overexpression restored endocytic recycling of GFP-Snc1p in the Cdc50p-depleted *dnf1*Δ *crf1*Δ cells. However, interestingly, expression of *GFP-SNC1* inhibited the suppression of growth defects by the *CHO1* overexpression (**Fig. 4D**). Consistently, endocytic recycling of GFP-Snc1p was not restored by the *CHO1* overexpression either (data not shown). This inhibitory effect was not observed with GFP-Snc1p(pm) (**Fig. 4D**). Since Snc1p is a cargo of a vesicle formed from early endosomes, these results may suggest that GFP-tagging of Snc1p interferes with some step in vesicle formation, which is promoted by PS increase.

I confirmed that PS content was increased from 14.2 ± 1.6% to 20.4 ± 0.2% in the Cdc50p-depleted *dnf1*Δ *crf1*Δ mutant by *CHO1* overexpression as in the Cdc50p-depleted *neo1-101* mutant (**Fig. 4E**). Unexpectedly, a slight decrease

in the PC level was observed from 43.0 ± 1.1% to 38.4 ± 1.5% for an unknown reason. A previous study showed that deletion of *PEM2* involved in PC synthesis decreased PC content from 41% to 37% (46). I examined whether the *pem2*Δ mutation suppressed the growth defect in the Cdc50p-depleted *dnf1*Δ *crf1*Δ mutant, but it did not (data not shown), suggesting that the PC decrease was not responsible for the suppression. Taken together, these results suggest that the defects of growth and endocytic recycling in flippase mutants could be suppressed by PS increase.

Suppression by PS increase seems to be dependent on a remaining flippase

My results suggest that increase of PS promotes vesicle formation from early endosomes in the flippase mutants. One possible mechanism is that increased PS is used by a remaining flippase to increase efficiency of flippase-mediated vesicle formation, whereas the other possibility is that PS in the outer leaflet of endosomal membranes is sufficient for vesicle formation by itself (e.g. PS recruits vesicle coat proteins). If the suppression is dependent on a flippase, it would not occur in the absence of flippases. I overexpressed *CHO1* in the Cdc50p-depleted *lem3*Δ *crf1*Δ mutant in which Drs2p, Dnf1p, Dnf2p, and Dnf3p are not functional, but *CHO1* weakly suppressed the growth defect (**Fig. 5A**). I reasoned that Neo1p might promote vesicle formation with increased PS in this

mutant, because Neo1p functioned with Drs2p in the endocytic recycling pathway as shown in Fig. 2. In fact, overexpression of *NEO1* suppressed the growth defect of the Cdc50p-depleted *lem3*Δ *crf1*Δ mutant, and co-overexpression of *CHO1* and *NEO1* enhanced this suppression (**Fig. 5A**). Then, I wanted to examine whether *CHO1* overexpression would suppress the growth defect in the Cdc50p- and Neo1p-depleted *lem3*Δ *crf1*Δ mutant. However, *CHO1* overexpression did not suppress the growth defect of even the Neo1p-depleted single mutant (**Fig. 5B**). This may be because Neo1p is involved in various cell functions other than the endocytic recycling pathway, including retrograde transport from Golgi to the ER (10) and membrane trafficking within the endosomal/Golgi system (11). Consistently, the growth defect of Neo1p-depleted cells was not suppressed by the overexpression of *CDC50/DRS2*, *CDC50/DRS2* and *CHO1*, or *LEM3/DNF1* (**Fig. 5B**).

I next examined the *neo1-101* allele, which seems to be specifically defective in the endocytic recycling pathway. The growth defect of the Cdc50p-depleted *neo1-101* mutant was suppressed by overexpression of *LEM3*/*DNF1* as well as *CHO1* (**Fig. 5C**). In addition, the suppression was enhanced by co-overexpression of *LEM3*/*DNF1* and *CHO1*. Dnf1p-GFP was normally localized to polarized plasma membrane sites as Dnf2p-GFP was, but in the Cdc50p-deleted *neo1-101* mutant, Dnf1p-GFP was localized to endosomal

membranes in which mRFP-Snc1p was accumulated (**Fig. 5D**). These results suggest that overexpressed Lem3p-Dnf1p supported vesicle formation from early endosomes in the Cdc50p-depleted *neo1-101* mutant, and that this vesicle formation was enhanced by PS increase.

Finally, the growth defect in the Cdc50p-depleted *neo1-101 lem3*Δ *crf1*Δ mutant was not suppressed by overexpression of *CHO1* (**Fig. 5E**). Thus, I concluded that the suppression of flippase mutations by increased PS was mediated by a remaining flippase.

PS is present in the cytoplasmic leaflet of early endosome membranes even in the absence of flippases

If PS in the cytoplasmic leaflet of early endosome membranes plays a direct role in vesicle formation, PS may not be found in the cytoplasmic leaflet of endosomal membranes that are accumulated in the flippase mutants. Distribution of PS in the cytoplasmic leaflet of the plasma membrane and internal membranes could be monitored with GFP-Lact-C2, the GFP-fused C2 domain of lactadherin, which specifically binds to PS (29).

In wild-type cells, GFP-Lact-C2 was exclusively localized to the plasma membrane and no intracellular localization was observed as reported previously (**Fig. 6A**) (29, 47). In contrast, in the Cdc50p-depleted *dnf1*Δ *crf1*Δ mutant,

GFP-Lact-C2 was also localized to endosomal membranes merged with mRFP-Snc1p (94%, n=100). This GFP-Lact-C2 signal was not observed with a mutant version of GFP-Lact-C2, GFP-Lact-C2-AAA, which does not bind to PS (29). I confirmed that expression of GFP-Lact-C2 did not affect the PS content in the Cdc50p-depleted *dnf1*Δ *crf1*Δ cells (**Fig. 6B**). Because it was possible that the PS in the cytoplasmic leaflet resulted from PS flipping by remaining flippases including Lem3p-Dnf2p and Neo1p, I examined localization of GFP-Lact-C2 in the mutant in which all known flippases are not functional, that is, the Cdc50p- and Neo1p-depleted *lem3*Δ *crf1*Δ mutant. GFP-Lact-C2 was again localized to the mRFP-Snc1p-containing membranes (98%, n=122) (**Fig. 6C**), although this mutant seems to accumulate TGN membranes in addition to endosomal membranes due to possible inhibition of the exocytosis pathway (data not shown).

These results seem to be consistent with expected transbilayer distribution of PS in early endosomes: PS enriched in the cytoplasmic leaflet of the plasma membrane would be exposed on the cytoplasmic leaflet of early endosomes after endocytosis and vesicle fusion with early endosomes unless PS is actively transported to the luminal leaflet (flopped) after endocytosis. It was previously shown that PS was actually present in the cytoplasmic leaflet of endocytic vesicles in yeast (48). In wild-type cells, however, no intracellular structures were visualized with GFP-Lact-C2 (**Fig. 6A**), suggesting that PS is not abundant

in the cytoplasmic leaflet of normal early endosomes. While yeast early endosomes are poorly characterized organelles with no specific marker protein identified, they may be too small to be visualized with GFP-Lact-C2 or PS in the cytoplasmic leaflet may be removed by efficient vesicle formation from early endosomes in wild-type cells.

My results suggest that the mere presence of PS in the cytoplasmic leaflet would not be enough for vesicle formation. Thus, I propose that PS has to be flipped by flippases from the luminal to the cytoplasmic leaflet when a vesicle is formed (e.g. PS flipping is coupled with vesicle formation). This luminal PS in early endosomes, which would not be supplied by endocytic vesicles, may be delivered by vesicle transport from TGN membranes.

PS is not essential for the endocytic recycling pathway

I next examined whether PS is essential for the early endosome to TGN retrieval pathway. Deletion of *CHO1* completely eliminates PS synthesis and depletes PS from these strains (49). In *cho1*Δ cells, GFP-Snc1p was normally localized to polarized plasma membrane sites as in wild-type cells (**Fig. 7A**), suggesting that the endocytic recycling pathway was not largely affected in *cho1*Δ cells. GFP-Snc1p(pm) was also exclusively localized at the plasma membrane in *cho1*Δ cells as in wild-type cells, consistent with a previous report that protein transport

and processing in the secretory pathway was normal in the *cho1*Δ mutant (12). In *cho1*Δ cells, the AP-1 β1 subunit, Apl2p-GFP, was localized to dotty structures that are endosomal/TGN membranes as in wild-type cells (50), indicating that PS is not essential for recruitment of AP-1 to these membranes. Taken together, these results suggest that PS is dispensable for the endocytic recycling pathway as well as for the secretory pathway.

To examine the impact of PS depletion on the Cdc50p-Drs2p function, I analyzed the *cdc50*Δ *cho1*Δ double mutant. As reported previously for the *drs2*Δ *cho1*Δ mutant (12), the *cdc50*Δ *cho1*Δ mutant exhibited a synthetic growth defect (**Fig. 7B**). This growth defect paralleled the defect in endocytic recycling of Dnf2p-GFP: Dnf2p-GFP was normally polarized in *cho1*Δ cells (83%, n=117 budded cells) and was significantly polarized in Cdc50p-depleted cells (34%, n=119), but not in Cdc50p-depleted *cho1*Δ cells (5%, n=104) (**Fig. 7C**). In the Cdc50p-depleted *cho1*Δ cells, Dnf2p-GFP was localized to membrane structures that were not colocalized with Sec7p-mRFP (**Fig. 7D**), suggesting that Cdc50p-Drs2p and Cho1p redundantly function in the endocytic recycling pathway.

I concluded that, although PS increase alleviates growth and endocytic recycling defects in flippase mutants and PS is involved in the flippase function, PS is not an essential phospholipid for the flippase-mediated vesicle formation

from early endosomes.

Increased PE also alleviates defects in the flippase mutants

The results described above suggest that, in the *cho1*Δ mutant, phospholipids other than PS are utilized by flippases to promote vesicle formation from early endosomes. Because PE is also a potential substrate of flippases (6, 9, 13), I next examined whether increased PE would suppress the defects in the flippase mutants. *PSD1* and *PSD2* encode PS decarboxylases that catalyze formation of PE from PS. Psd1p is engaged in mitochondrial PE biosynthesis (51, 52), while Psd2p is implicated in PE synthesis in endosomal/TGN membranes (53, 54). As shown in **Fig. 8A**, overexpression of *PSD2* weakly suppressed the growth defect of Cdc50p-depleted *dnf1*Δ *crf1*Δ as well as Cdc50p-depleted *neo1-101* cells, although this suppression was observed in synthetic (SDA) medium, but not in rich (YPD) medium (data not shown). I confirmed that the total cellular PE content was increased from 18.3 ± 1.6% to 22.4 ± 1.5% and from 19.9 ± 2.1% to 23.5 ± 1.9% by *PSD2* in the Cdc50p-depleted *neo1-101* and Cdc50p-depleted *dnf1*Δ *crf1*Δ cells, respectively (**Fig. 8B**). Consistent with the weak suppression of growth defects, cells with polarized Dnf2p-GFP were slightly increased from 11.5 ± 3.0% to 23.0 ± 3.2% by *PSD2* overexpression in the Cdc50p-depleted *dnf1*Δ *crf1*Δ cells (four independent experiments, *t*-test *P<0.05) (data not

shown).

I next examined whether PE is required for endocytic recycling of GFP-Snc1p. Although complete depletion of PE results in lethality, the *psd1*Δ *psd2*Δ mutant is viable, because Dpl1p coding for dihydrosphingosine-1-phosphate lyase permits low levels of PE synthesis (55, 56). In the *psd1*Δ *psd2*Δ mutant, PE content was markedly decreased to 2.2 ± 0.2% from 16.6 ± 1.4% in the wild-type (**Fig. 8C**). However, GFP-Snc1p was normally localized to polarized sites in the *psd1*Δ *psd2*Δ mutant (**Fig. 8D**). In addition, the *psd1*Δ *psd2*Δ *cdc50*Δ mutant did not exhibit synthetic defects in growth and endocytic recycling of GFP-Snc1p (data not shown). These results suggest that the low level of PE does not cause a defect in the flippase-mediated vesicle formation from early endosomes.

Taken together, my results raise the possibility that, in addition to PS, PE could be also utilized by flippases to promote vesicle formation from early endosomes in the early endosome-to TGN pathway.

Discussion

In this work I demonstrate that increase of PS by overexpression of *CHO1* alleviates defects in growth and endocytic recycling of flippase mutants (Fig. 3-5). Many studies using a fluorescence-labeled phospholipid analogue or a lipid-binding peptide suggested that flippases translocate phospholipids, but it needs to be demonstrated that flippases act on endogenous phospholipids. My results provide genetic evidence for the functional relevance between flippases and endogenous phospholipids.

Neo1p is distinct from other flippases in that it is an essential protein and does not associate with a Cdc50p family member. Isolation and characterization of the *neo1-101* mutant suggested that Neo1p is involved in the endocytic recycling pathway (Fig. 2). *NEO1* was previously isolated as a multicopy suppressor of the *cdc50-11 lem3*Δ *crf1*Δ mutant (7). Although Neo1p has not been demonstrated to possess a flippase activity, these results imply that Neo1p functions as a flippase like other flippases.

Overexpression of *CHO1* caused two opposite effects in the phospholipid content: increase of PS and decrease of PI (Fig. 3D, 4E). Although I cannot exclude a possibility that decrease of PI is involved in the suppression, increase of PS, a known substrate of flippases, seems to be responsible, because the suppression was dependent on remaining flippases (Fig. 5). Thus, it was

suggested that increased PS was flipped by the flippases to promote vesicle formation from early endosomes. The *cdc50*Δ mutation exhibited synthetic defects with *cho1*Δ (Fig. 7), but not with *psd1*Δ *psd2*Δ, suggesting that PS is functionally more relevant to flippases than PE. Since PS has been suggested to be a preferable substrate of Drs2p *in vitro* (12, 14), PS seems to be more effective in Drs2p-mediated vesicle formation compared with other phospholipids. In contrast, it has not been clearly demonstrated that Lem3p-Dnf1/2p flips PS: NBD-labeled PS was still flipped in the *lem3*Δ mutant probably due to an unidentified protein on the plasma membrane (57), and NBD-PS was a less preferred substrate of Dnf1p compared with NBD-PC and NBD-PE (58). However, growth of the *lem3*Δ mutant was clearly sensitive to papuamide B, a cyclic lipopeptide that shows cytotoxicity by binding to PS in biological membranes (59), and this sensitivity was suppressed by the *cho1*Δ mutation (data not shown), indicating that PS is exposed on the cell surface in this mutant. These results may suggest that Lem3p-Dnf1/2p flips PS more efficiently than NBD-PS.

Two possible mechanisms could be envisioned on how increased PS enhances vesicle formation (**Fig. 9**). One is that flipped PS in the cytoplasmic leaflet recruits adaptor or coat proteins for vesicle formation with its negative charge. PS has been suggested to be an important factor for directing endocytic proteins to the plasma membrane (60). In the *cdc50*Δ and *rcy1*Δ mutants, in which

early endosomal membranes are intracellularly accumulated, endocytic proteins were assembled on those membranes, probably in a PS-dependent manner (60, 61). In mammalian cells, PS in recycling endosomes recruited evectin-2 *via* interaction with the pleckstrin homology (PH) domain (62). However, GFP-Lact-C2 detected PS in the cytoplasmic leaflet of early endosome membranes in flippase mutants (Fig. 6). This PS seems to be transported from the plasma membrane through the endocytosis-recycling route (60). These results suggest that the presence of PS in the cytoplasmic leaflet is not sufficient for vesicle formation.

Thus, I favor the other mechanism: PS flipping by a flippase induces a local membrane curvature that assists in vesicle formation (21). Elucidation of how this membrane curvature is harnessed to form a vesicle is a next challenge. Proteins containing an amphipathic lipid packing sensor (ALPS) motif (63) are candidates that recognize the flippase-induced membrane curvature. It was previously shown that the Arf1p GTPase activating protein gene *GCS1* genetically interacts with *CDC50* (18), and have recently shown that its ALPS motif is involved in this functional interaction (64). More recently, Gcs1p has been proposed to be an effector that recognizes the membrane curvature induced by Cdc50p-Drs2p through its ALPS motif (65). However, the endocytic recycling defects in the *gcs1*Δ mutant is negligible compared to the *cdc50*Δ/*drs2*Δ mutant

(data not shown), indicating that there should be another protein that recognizes the membrane curvature formed by Cdc50p-Drs2p.

Although PS has been suggested to be a preferable substrate of Drs2p *in vitro* (12, 14), the endocytic recycling pathway was not totally dependent on PS. Endocytic recycling was not significantly affected in the *cho1*Δ mutant, but severely impaired in the *cho1*Δ *cdc50*Δ mutant (Fig. 7), indicating that Cdc50p-Drs2p has a function(s) in the endocytic recycling pathway in the absence of PS. Cdc50p-Drs2p might perform a flippase-independent function as suggested for mammalian ATP8B1 flippase (66), but another interesting possibility is that Cdc50p-Drs2p flips PE as suggested previously (6, 13) to form a vesicle in the absence of PS.

Similar to PS, increased PE alleviated the growth defect of the Cdc50p-depleted *neo1-101* and *dnf1*Δ *crf1*Δ mutants, which contain Lem3p-Dnf1/2p and Lem3p-Dnf2p, respectively (Fig. 8). These flippases may utilize increased PE to form a vesicle, because Lem3p-Dnf1/2p have been suggested to translocate a fluorescently labeled PE and PC (9, 15). Interestingly, simultaneous depletion of PS and PE (*cho1*Δ cells grown in SD medium supplemented with 2 mM choline) did not cause an obvious recycling defect (data not shown). It is possible that Lem3p-Dnf1/2p also flip PC in the absence of both PS and PE to form a vesicle from early endosomes.

Because both Cdc50p-Drs2p and Lem3p-Dnf1/2p are involved in the endocytic recycling pathway, it seems reasonable to suppose that PE/PC flipping contributes to flippase-mediated vesicle formation, albeit with reduced efficiency compared to PS. This is also consistent with my notion that flippase-mediated vesicle formation is promoted by membrane curvature rather than chemical or physical properties of a specific phospholipid.

References

1. **Lenoir G, Williamson P, Holthuis JC.** 2007. On the origin of lipid asymmetry: the flip side of ion transport. Curr Opin Chem Biol **11:**654-661.

2. **Sebastian TT, Baldridge RD, Xu P, Graham TR.** 2012. Phospholipid flippases: building asymmetric membranes and transport vesicles. Biochim Biophys Acta **1821:**1068-1077.

3. **Tanaka K, Fujimura-Kamada K, Yamamoto T.** 2011. Functions of phospholipid flippases. J Biochem **149:**131-143.

4. **Daleke DL.** 2007. Phospholipid flippases. J Biol Chem **282:**821-825.

5. **van der Mark VA, Elferink RP, Paulusma CC.** 2013. P4 ATPases: Flippases in Health and Disease. Int J Mol Sci **14:**7897-7922.

6. **Saito K, Fujimura-Kamada K, Furuta N, Kato U, Umeda M, Tanaka K.** 2004. Cdc50p, a protein required for polarized growth, associates with the Drs2p P-type ATPase implicated in phospholipid translocation in *Saccharomyces cerevisiae*. Mol Biol Cell **15:**3418-3432.

7. **Furuta N, Fujimura-Kamada K, Saito K, Yamamoto T, Tanaka K.** 2007. Endocytic recycling in yeast is regulated by putative phospholipid translocases and the Ypt31p/32p-Rcy1p pathway. Mol Biol Cell **18:**295-312.

8. **Hua Z, Fatheddin P, Graham TR.** 2002. An essential subfamily of Drs2p-related P-type ATPases is required for protein trafficking between Golgi complex and endosomal/vacuolar system. Mol Biol Cell **13:**3162-3177.

9. **Pomorski T, Lombardi R, Riezman H, Devaux PF, van Meer G, Holthuis JC.** 2003. Drs2p-related P-type ATPases Dnf1p and Dnf2p are required for phospholipid translocation across the yeast plasma membrane and serve a role in endocytosis. Mol Biol Cell **14:**1240-1254.

10. **Hua Z, Graham TR.** 2003. Requirement for neo1p in retrograde transport from the Golgi complex to the endoplasmic reticulum. Mol Biol Cell **14:**4971-4983.

11. **Wicky S, Schwarz H, Singer-Krüger B.** 2004. Molecular interactions of yeast Neo1p, an essential member of the Drs2 family of aminophospholipid translocases, and its role in membrane trafficking within the endomembrane system. Mol Cell Biol **24:**7402-7418.

12. **Natarajan P, Wang J, Hua Z, Graham TR.** 2004. Drs2p-coupled aminophospholipid translocase activity in yeast Golgi membranes and relationship to in vivo function. Proc Natl Acad Sci U S A **101:**10614-10619.

13. **Alder-Baerens N, Lisman Q, Luong L, Pomorski T, Holthuis JC.** 2006. Loss of P4 ATPases Drs2p and Dnf3p disrupts aminophospholipid transport and asymmetry in yeast post-Golgi secretory vesicles. Mol Biol Cell **17:**1632-1642.

14. **Zhou X, Graham TR.** 2009. Reconstitution of phospholipid translocase activity with purified Drs2p, a type-IV P-type ATPase from budding yeast. Proc Natl Acad Sci U S A **106:**16586-16591.

15. **Kato U, Emoto K, Fredriksson C, Nakamura H, Ohta A, Kobayashi T, Murakami-Murofushi K, Umeda M.** 2002. A novel membrane protein, Ros3p, is required for phospholipid translocation across the plasma membrane in *Saccharomyces cerevisiae*. J Biol Chem **277:**37855-37862.

16. **Chen CY, Ingram MF, Rosal PH, Graham TR.** 1999. Role for Drs2p, a P-type ATPase and potential aminophospholipid translocase, in yeast late Golgi function. J Cell Biol **147:**1223-1236.

17. **Gall WE, Geething NC, Hua Z, Ingram MF, Liu K, Chen SI, Graham TR.** 2002. Drs2p-dependent formation of exocytic clathrin-coated vesicles *in vivo*. Curr Biol **12:**1623-1627.

18. **Sakane H, Yamamoto T, Tanaka K.** 2006. The functional relationship between the Cdc50p-Drs2p putative aminophospholipid translocase and the Arf GAP Gcs1p in vesicle formation in the retrieval pathway from yeast early endosomes to the TGN. Cell Struct Funct **31:**87-108.

19. **Liu K, Surendhran K, Nothwehr SF, Graham TR.** 2008. P4-ATPase requirement for AP-1/clathrin function in protein transport from the *trans*-Golgi network and early endosomes. Mol Biol Cell **19:**3526-3535.

20. **Kelly BT, Owen DJ.** 2011. Endocytic sorting of transmembrane protein cargo. Curr Opin Cell Biol **23:**404-412.

21. **Graham TR, Kozlov MM.** 2010. Interplay of proteins and lipids in generating membrane curvature. Curr Opin Cell Biol **22:**430-436.

22. **Rose MD, Winston, F., and Hieter, P.** 1990. Methods in Yeast Genetics: A Laboratory Course Manual. Cold Spring Harbor Laboratory Press, Cold Spring Harbor, NY.

23. **Guthrie C.** 1991. Guide to Yeast Genetics and Molecular Biology. *In* Fink GR (ed.). Methods Enzymol. 194, Academic Press, San Diego, CA.

24. **Gietz RD, Woods RA.** 2002. Transformation of yeast by lithium acetate/single-stranded carrier DNA/polyethylene glycol method. Methods Enzymol **350:**87-96.

25. **Elble R.** 1992. A simple and efficient procedure for transformation of yeasts. Biotechniques **13:**18-20.

26. **Longtine MS, McKenzie A, Demarini DJ, Shah NG, Wach A, Brachat A, Philippsen P, Pringle JR.** 1998. Additional modules for versatile and economical PCR-based gene deletion and modification in *Saccharomyces cerevisiae*. Yeast **14:**953-961.

27. **Hachiro T, Yamamoto T, Nakano K, Tanaka K.** 2013. Phospholipid flippases Lem3p-Dnf1p and Lem3p-Dnf2p are involved in the sorting of the tryptophan permease Tat2p in yeast. J Biol Chem **288:**3594-3608.

28. **Goldstein AL, McCusker JH.** 1999. Three new dominant drug resistance cassettes for gene disruption in *Saccharomyces cerevisiae*. Yeast **15:**1541-1553.

29. **Yeung T, Gilbert GE, Shi J, Silvius J, Kapus A, Grinstein S.** 2008. Membrane phosphatidylserine regulates surface charge and protein localization. Science **319:**210-213.

30. **Ho SN, Hunt HD, Horton RM, Pullen JK, Pease LR.** 1989. Site-directed mutagenesis by overlap extension using the polymerase chain reaction. Gene **77:**51-59.

31. **Ma H, Kunes S, Schatz PJ, Botstein D.** 1987. Plasmid construction by homologous recombination in yeast. Gene **58:**201-216.

32. **Botstein D, Falco SC, Stewart SE, Brennan M, Scherer S, Stinchcomb DT, Struhl K, Davis RW.** 1979. Sterile host yeasts (SHY): a eukaryotic system of biological containment for recombinant DNA experiments. Gene **8:**17-24.

33. **Bligh EG, Dyer WJ.** 1959. A rapid method of total lipid extraction and purification. Can J Biochem Physiol **37:**911-917.

34. **Schüller C, Mamnun YM, Wolfger H, Rockwell N, Thorner J, Kuchler K.** 2007. Membrane-active compounds activate the transcription factors Pdr1 and Pdr3 connecting pleiotropic drug resistance and membrane lipid homeostasis in *Saccharomyces cerevisiae*. Mol Biol Cell **18:**4932-4944.

35. **Weerheim AM, Kolb AM, Sturk A, Nieuwland R.** 2002. Phospholipid composition of cell-derived microparticles determined by one-dimensional high-performance thin-layer chromatography. Anal Biochem **302:**191-198.

36. **Nakano K, Yamamoto T, Kishimoto T, Noji T, Tanaka K.** 2008. Protein kinases Fpk1p and Fpk2p are novel regulators of phospholipid asymmetry. Mol Biol Cell **19:**1783-1797.

37. **Takagi K, Iwamoto K, Kobayashi S, Horiuchi H, Fukuda R, Ohta A.** 2012. Involvement of Golgi-associated retrograde protein complex in the recycling of the putative Dnf aminophospholipid flippases in yeast. Biochem Biophys Res Commun **417:**490-494.

38. **Lewis MJ, Nichols BJ, Prescianotto-Baschong C, Riezman H, Pelham HR.** 2000. Specific retrieval of the exocytic SNARE Snc1p from early yeast endosomes. Mol Biol Cell **11:**23-38.

39. **Holthuis JC, Nichols BJ, Dhruvakumar S, Pelham HR.** 1998. Two syntaxin homologues in the TGN/endosomal system of yeast. EMBO J **17:**113-126.

40. **Siniossoglou S, Pelham HR.** 2001. An effector of Ypt6p binds the SNARE Tlg1p and mediates selective fusion of vesicles with late Golgi membranes. EMBO J **20:**5991-5998.

41. **Carman GM, Han GS.** 2011. Regulation of phospholipid synthesis in the yeast *Saccharomyces cerevisiae*. Annu Rev Biochem **80:**859-883.

42. **Shindiapina P, Barlowe C.** 2010. Requirements for transitional endoplasmic reticulum site structure and function in *Saccharomyces cerevisiae*. Mol Biol Cell **21:**1530-1545.

43. **Letts VA, Klig LS, Bae-Lee M, Carman GM, Henry SA.** 1983. Isolation of the yeast structural gene for the membrane-associated enzyme phosphatidylserine synthase. Proc Natl Acad Sci U S A **80:**7279-7283.

44. **Gardocki ME, Jani N, Lopes JM.** 2005. Phosphatidylinositol biosynthesis: biochemistry and regulation. Biochim Biophys Acta **1735:**89-100.

45. **Williams JG, McMaster CR.** 1998. Scanning alanine mutagenesis of the CDP-alcohol phosphotransferase motif of *Saccharomyces cerevisiae* cholinephosphotransferase. J Biol Chem **273:**13482-13487.

46. **Gohil VM, Thompson MN, Greenberg ML.** 2005. Synthetic lethal interaction of the mitochondrial phosphatidylethanolamine and cardiolipin biosynthetic pathways in *Saccharomyces cerevisiae*. J Biol Chem **280:**35410-35416.

47. **Fairn GD, Hermansson M, Somerharju P, Grinstein S.** 2011. Phosphatidylserine is polarized and required for proper Cdc42 localization and for development of cell polarity. Nat Cell Biol **13:**1424-1430.

48. **Pranke IM, Morello V, Bigay J, Gibson K, Verbavatz JM, Antonny B, Jackson CL.** 2011. α-Synuclein and ALPS motifs are membrane curvature sensors whose contrasting chemistry mediates selective vesicle binding. J Cell Biol **194:**89-103.

49. **Atkinson K, Fogel S, Henry SA.** 1980. Yeast mutant defective in phosphatidylserine synthesis. J Biol Chem **255:**6653-6661.

50. **Costaguta G, Duncan MC, Fernández GE, Huang GH, Payne GS.** 2006. Distinct roles for TGN/endosome epsin-like adaptors Ent3p and Ent5p. Mol Biol Cell **17:**3907-3920.

51. **Trotter PJ, Pedretti J, Voelker DR.** 1993. Phosphatidylserine decarboxylase from *Saccharomyces cerevisiae*. Isolation of mutants, cloning of the gene, and creation of a null allele. J Biol Chem **268:**21416-21424.

52. **Clancey CJ, Chang SC, Dowhan W.** 1993. Cloning of a gene (*PSD1*) encoding phosphatidylserine decarboxylase from *Saccharomyces cerevisiae* by complementation of an *Escherichia coli* mutant. J Biol Chem **268:**24580-24590.

53. **Gulshan K, Shahi P, Moye-Rowley WS.** 2010. Compartment-specific synthesis of phosphatidylethanolamine is required for normal heavy metal resistance. Mol Biol Cell **21:**443-455.

54. **Trotter PJ, Voelker DR.** 1995. Identification of a non-mitochondrial phosphatidylserine decarboxylase activity (*PSD2*) in the yeast *Saccharomyces cerevisiae*. J Biol Chem **270:**6062-6070.

55. **Saba JD, Nara F, Bielawska A, Garrett S, Hannun YA.** 1997. The *BST1* gene of *Saccharomyces cerevisiae* is the sphingosine-1-phosphate lyase. J Biol Chem **272:**26087-26090.

56. **Storey MK, Clay KL, Kutateladze T, Murphy RC, Overduin M, Voelker DR.** 2001. Phosphatidylethanolamine has an essential role in *Saccharomyces cerevisiae* that is independent of its ability to form hexagonal phase structures. J Biol Chem **276:**48539-48548.

57. **Stevens HC, Malone L, Nichols JW.** 2008. The putative aminophospholipid translocases, DNF1 and DNF2, are not required for 7-nitrobenz-2-oxa-1,3-diazol-4-yl-phosphatidylserine flip across the plasma membrane of *Saccharomyces cerevisiae*. J Biol Chem **283:**35060-35069.

58. **Baldridge RD, Graham TR.** 2012. Identification of residues defining phospholipid flippase substrate specificity of type IV P-type ATPases. Proc Natl Acad Sci U S A **109:**E290-298.

59. **Parsons AB, Lopez A, Givoni IE, Williams DE, Gray CA, Porter J, Chua G, Sopko R, Brost RL, Ho CH, Wang J, Ketela T, Brenner C, Brill JA, Fernandez GE, Lorenz TC, Payne GS, Ishihara S, Ohya Y, Andrews B, Hughes TR, Frey BJ, Graham TR, Andersen RJ, Boone C.** 2006. Exploring the mode-of-action of bioactive compounds by chemical-genetic profiling in yeast. Cell **126:**611-625.

60. **Sun Y, Drubin DG.** 2012. The functions of anionic phospholipids during clathrin-mediated endocytosis site initiation and vesicle formation. J Cell Sci **125:**6157-6165.

61. **Kishimoto T, Yamamoto T, Tanaka K.** 2005. Defects in structural integrity of ergosterol and the Cdc50p-Drs2p putative phospholipid

translocase cause accumulation of endocytic membranes, onto which actin patches are assembled in yeast. Mol Biol Cell **16:**5592-5609.

62. **Uchida Y, Hasegawa J, Chinnapen D, Inoue T, Okazaki S, Kato R, Wakatsuki S, Misaki R, Koike M, Uchiyama Y, Iemura S, Natsume T, Kuwahara R, Nakagawa T, Nishikawa K, Mukai K, Miyoshi E, Taniguchi N, Sheff D, Lencer WI, Taguchi T, Arai H.** 2011. Intracellular phosphatidylserine is essential for retrograde membrane traffic through endosomes. Proc Natl Acad Sci U S A **108:**15846-15851.

63. **Antonny B.** 2011. Mechanisms of membrane curvature sensing. Annu Rev Biochem **80:**101-123.

64. **Zendeh-boodi Z, Yamamoto T, Sakane H, Tanaka K.** 2013. Identification of a second amphipathic lipid-packing sensor-like motif that contributes to Gcs1p function in the early endosome-to-TGN pathway. J Biochem **153:**573-587.

65. **Xu P, Baldridge RD, Chi RJ, Burd CG, Graham TR.** 2013. Phosphatidylserine flipping enhances membrane curvature and negative charge required for vesicular transport. J Cell Biol **202:**875-886.

66. **Verhulst PM, van der Velden LM, Oorschot V, van Faassen EE, Klumperman J, Houwen RH, Pomorski TG, Holthuis JC, Klomp LW.** 2010. A flippase-independent function of ATP8B1, the protein affected in familial intrahepatic cholestasis type 1, is required for apical protein expression and microvillus formation in polarized epithelial cells. Hepatology **51:**2049-2060.

67. **Noji T, Yamamoto T, Saito K, Fujimura-Kamada K, Kondo S, Tanaka K.** 2006. Mutational analysis of the Lem3p-Dnf1p putative phospholipid-translocating P-type ATPase reveals novel regulatory roles

for Lem3p and a carboxyl-terminal region of Dnf1p independent of the phospholipid-translocating activity of Dnf1p in yeast. Biochem Biophys Res Commun **344:**323-331.

68. **Sikorski RS, Hieter P.** 1989. A system of shuttle vectors and yeast host strains designed for efficient manipulation of DNA in *Saccharomyces cerevisiae*. Genetics **122:**19-27.

69. **Gietz RD, Sugino A.** 1988. New yeast-*Escherichia coli* shuttle vectors constructed with *in vitro* mutagenized yeast genes lacking six-base pair restriction sites. Gene **74:**527-534.

Acknowledgments

I would like to give heartfelt thanks to Dr. Kazuma Tanaka whose enormous support and insightful comments were invaluable during the course of my study. I am also indebted to Dr. Takamitsu Sano, Eriko Itoh and my peers who provided technical help and sincere encouragement. I would also like to express my gratitude to my family for their moral support and warm encouragements.

Table 1 Yeast strains used in this study

Strain*	Relevant genotype	Derivation/source
YEF473	*MATa/α lys2-801/lys2-801 ura3-52/ira3-52 his3Δ-200/his3Δ-200 trp1Δ-63/trp1Δ-63 leu2Δ-1/leu2Δ-1*	(26)
YKT1066	*MATa lys2-801 ura3-52 his3Δ-200 leu2Δ-1TRP1*	This study
YKT1651	*MATa neo1-101*	This study
YKT1781	*MATa neo1-101::LEU2 TRP1*	This study
YKT1782	*MATa KanMX6::P_{GAL1}-3HA-CDC50 TRP1*	This study
YKT1783	*MATa HphMX4::P_{GAL1}-3HA-CDC50 neo1-101::LEU2 TRP1*	This study
YKT1629	*MATa TRP1::P_{GAL1}-DRS2*	This study
YKT1784	*MATa TRP1::PGAL1-DRS2 neo1-101*	This study
YKT1785	*MATa DNF2-EGFP::natMX TRP1*	This study
YKT1786	*MATa neo1-101::LEU2 DNF2-EGFP::natMX TRP1*	This study
YKT1787	*MATα KanMX6::P_{GAL1}-3HA-CDC50 DNF2-EGFP::KanMX6 TRP1*	This study
YKT1788	*MATa HphMX4::P_{GAL1}-3HA-CDC50 neo1-101::LEU2 DNF2-EGFP::natMX TRP1*	This study
YKT1777	*MATα LEU2::mRFP-SNC1 TRP1*	This study
YKT1789	*MATa HphMX4::P_{GAL1}-3HA-CDC50 neo1-101::LEU2 LEU2::mRFP-SNC1 TRP1*	This study
YKT1790	*MATα HphMX4::P_{GAL1}-3HA-CDC50 neo1-101::LEU2 SEC7-mRFP::KanMX6 TRP1*	This study
YKT1650	*MATα HIS3MX6::P_{GAL1}-3HA-CDC50 neo1-101*	This study
YKT1529	*MATa KanMX6::P_{GAL1}-3HA-CDC50 dnf1Δ::HIS3MX6 crf1Δ::HphMX3 TRP1*	This study
YKT1791	*MATa KanMX6::P_{GAL1}-3HA-CDC50 dnf1Δ::HIS3MX6 crf1Δ::HphMX3 DNF2-EGFP::KanMX6 TRP1*	This study
YKT1792	*MATa KanMX6::P_{GAL1}-3HA-CDC50 dnf1Δ::HIS3MX6 crf1Δ::HphMX3 LEU2::GFP-SNC1 TRP1*	This study
YKT1793	*MATα TRP1::P_{GAL1}-3HA-CDC50 dnf1Δ::HIS3MX6*	This study

	crf1Δ:HphMX3 LEU2::GFP-SNC1(pm)	
YKT1513	*MATa KanMX6::P_{GAL1}-3HA-CDC50 lem3Δ::HIS3MX6 crf1Δ::HphMX3 TRP1*	This study
YKT1660	*MATa KanMX6::P_{GAL1}-3HA-NEO1*	This study
YKT1796	*MATα HphMX4::P_{GAL1}-3HA-CDC50 neo1-101::LEU2 lem3Δ::HIS3MX6 crf1Δ::HphMX4 TRP1*	This study
YKT1797	*MATa DNF1-EGFP::KanMX6 TRP1*	(67)
YKT1798	*MATα HphMX4::P_{GAL1}-3HA-CDC50 neo1-101::LEU2 DNF1-EGFP::KanMX6 TRP1*	This study
YKT1799	*MATa LEU2::GFP-Lact-C2 TRP1*	This study
YKT1800	*MATa KanMX6::P_{GAL1}-3HA-CDC50 dnf1Δ::HIS3MX6 crf1Δ::HphMX3 LEU2::GFP-Lact-C2 TRP1*	This study
YKT1801	*MATα KanMX6::P_{GAL1}-3HA-CDC50 dnf1Δ::HIS3MX6 crf1Δ::HphMX3 LEU2::mRFP-SNC1 URA3::GFP-Lact-C2-AAA TRP1*	This study
YKT1802	*MATa KanMX6::P_{GAL1}-3HA-CDC50 KanMX6::P_{GAL1}-3HA-NEO1 lem3Δ::HIS3MX6 crf1Δ::HphMX3 URA3::GFP-Lact-C2 TRP1*	This study
YKT1428	*MATa cho1Δ::KanMX4 TRP1*	This study
YKT1642	*MATa APL2-EGFP::KanMX6 TRP1*	This study
YKT1803	*MATa cho1Δ::natMX APL2-EGFP::KanMX6 TRP1*	This study
YKT1507	*MATa cdc50Δ::HIS3MX6 TRP1*	This study
YKT1804	*MATa cdc50Δ::HphMX4 cho1Δ::KanMX4 TRP1*	This study
YKT1805	*MATa DNF2-EGFP::HphMX4 TRP1*	This study
YKT1806	*MATα cho1Δ::natMX DNF2-EGFP::KanMX6 TRP1*	This study
YKT1807	*MATα KanMX6::P_{GAL1}-3HA-CDC50 cho1Δ::natMX DNF2-EGFP::KanMX6 TRP1*	This study
YKT1808	*MATα KanMX6::P_{GAL1}-3HA-CDC50 cho1Δ::natMX SEC7-mRFP::KanMX6 DNF2-GFP::HphMX4 TRP1*	This study
YKT1809	*MATa psd1Δ::KanMX6 psd2Δ::HIS3MX6 TRP1*	This study
YKT1523	*MATa URA3::GFP-SNC1 TRP1*	(64)

YKT1810	*MATa psd1Δ::KanMX6 psd2Δ::HIS3MX6 URA3::GFP-SNC1 TRP1*	This study
YKT1871	*MATa SEC63-mRFP::KanMX6 TRP1*	This study
YKT1872	*MATa HphMX4:: P_{GAL1}-3HA-CDC50 neo1-101::LEU2 SEC63-mRFP::KanMX6 TRP1*	This study

*YKT strains are isogenic derivatives of YEF473.

Table 2 Plasmids used in this study

Plasmid	Characteristics	Derivation / source
YEp24	*URA3 2µm*	(32)
pRS425	*LEU2 2µm*	(68)
YEplac112	*TRP1 2µm*	(69)
YEplac181	*LEU2 2µm*	(69)
YEplac195	*URA3 2µm*	(69)
pKT1488 [pRS416-GFP-TLG1]	P_{TPI1}*-GFP-TLG1 URA3 CEN*	This study
pKT1443 [pRS416-GFP-SNC1]	P_{TPI1}*-GFP-SNC1 URA3 CEN*	(38)
pKT1753 [YEp24-CHO1]	*CHO1 URA3 2µm*	This study
pKT1263 [YEplac195-CDC50]	*CDC50 URA3 2µm*	This study
pKT1964 [pRS416-mRFP-SNC1(pm)]	P_{TPI1}*-mRFP-SNC1(pm) URA3 CEN*	This study
pKT1788 [pRS425-NEO1]	*NEO1 LEU2 2µm*	This study
pKT2097 [YEplac112-CHO1]	*CHO1 TRP1 2µm*	This study
PKT2098 [YEplac112-LEM3]	*LEM3 TRP1 2µm*	This study
pKT1607 [YEplac195-DRS2-CDC50]	*DRS2-CDC50 URA3 2µm*	(6)
pKT1469 [YEplac195-NEO1]	*NEO1 URA3 2µm*	This study
pKT1602 [YEplac195-DNF1]	*DNF1 URA3 2µm*	(67)
pKT1340 [YEplac181-LEM3]	*LEM3 LEU2 2µm*	(67)
pKT1264 [YCplac22-CDC50]	*CDC50 TRP1 CEN*	This study
pKT1563 [pRS416-mRFP-SNC1]	P_{TPI1}*-mRFP-SNC1 URA3 CEN*	(61)
pKT1568 [pRS315-mRFP-SNC1]	P_{TPI1}*-mRFP-SNC1 LEU2 CEN*	This study
pKT1444 [pRS416-GFP-SNC1(pm)]	P_{TPI1}*-GFP-SNC1(pm) URA3 CEN*	(38)
pKT2096 [YEp352-PSD2]	*PSD2 URA3 2µm*	(53)
pKT2099 [pRS305-mRFP-SNC1]	P_{TPI1}*-mRFP-SNC1 LEU2*	This study
pKT1749 [pRS416-GFP-Lact-C2]	*GFP-Lact-C2 URA3 CEN*	(29)
pKT2100 [pRS306-GFP-Lact-C2]	*GFP-Lact-C2 URA3*	This study
pKT1995	*GFP-Lact-C2-AAA URA3*	This study

[pRS306-GFP-Lact-C2-AAA]		
pKT1807 [pRS316-NEO1]	*NEO1 URA3 CEN*	This study
pKT2102 [pRS305-neo1-101-C]	*neo1-101-C LEU2*	This study
pKT2101 [pRS305-GFP-Snc1(pm)]	P_{TPI1}*-GFP-SNC1(pm) LEU2*	This study
pKT2102 [pRS316-NEO1ΔBglII]	*NEO1ΔBglII URA3 CEN*	This study
pKT2111 [YEplac195-CHO1]	*CHO1 URA3*	This study
pKT2112 [YEplac195-CHO1-GFP]	*CHO1-GFP URA3*	This study
pKT2114 [YEplac195-CHO1 (D148A)]	*cho1(D148A) URA3*	This study
pKT2115 [YEplac195-CHO1 (D152A)]	*cho1(D152A) URA3*	This study

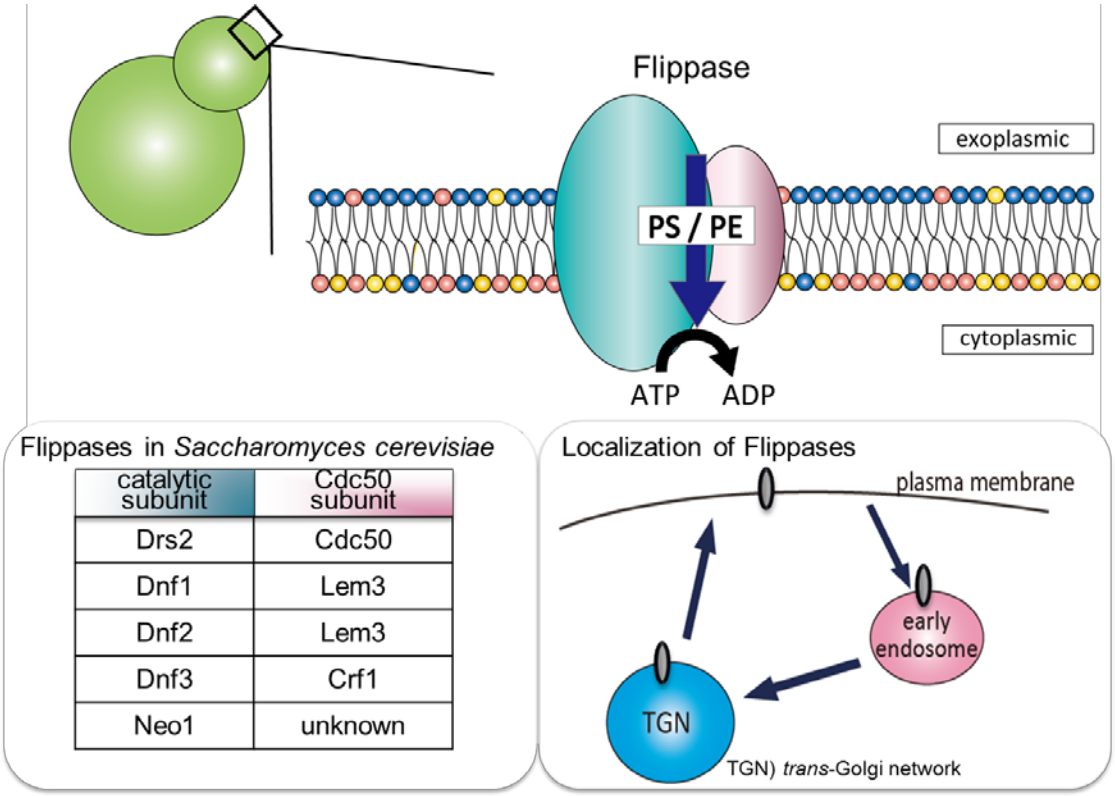

Figure 1. Flippases in *Saccharomyces cerevisiae* and the localization of flippases. Phospholipid flippases translocate phospholipids (PS and PE) from the exoplasmic to the cytoplasmic leaflet of cell membranes to generate and maintain phospholipid asymmetry. The genome of budding yeast encodes four heteromeric flippases (Drs2p, Dnf1p, Dnf2p, and Dnf3p), which associate with the Cdc50 family non-catalytic subunit, and one monomeric flippase Neo1p. Cdc50p-Drs2p, Lem3p-Dnf1/2p, and Crf1p-Dnf3p are recycled from the plasma membrane through early endosomes and the TGN back to the plasma membrane, and they have redundant roles in the early-endosome to TGN recycling pathway.

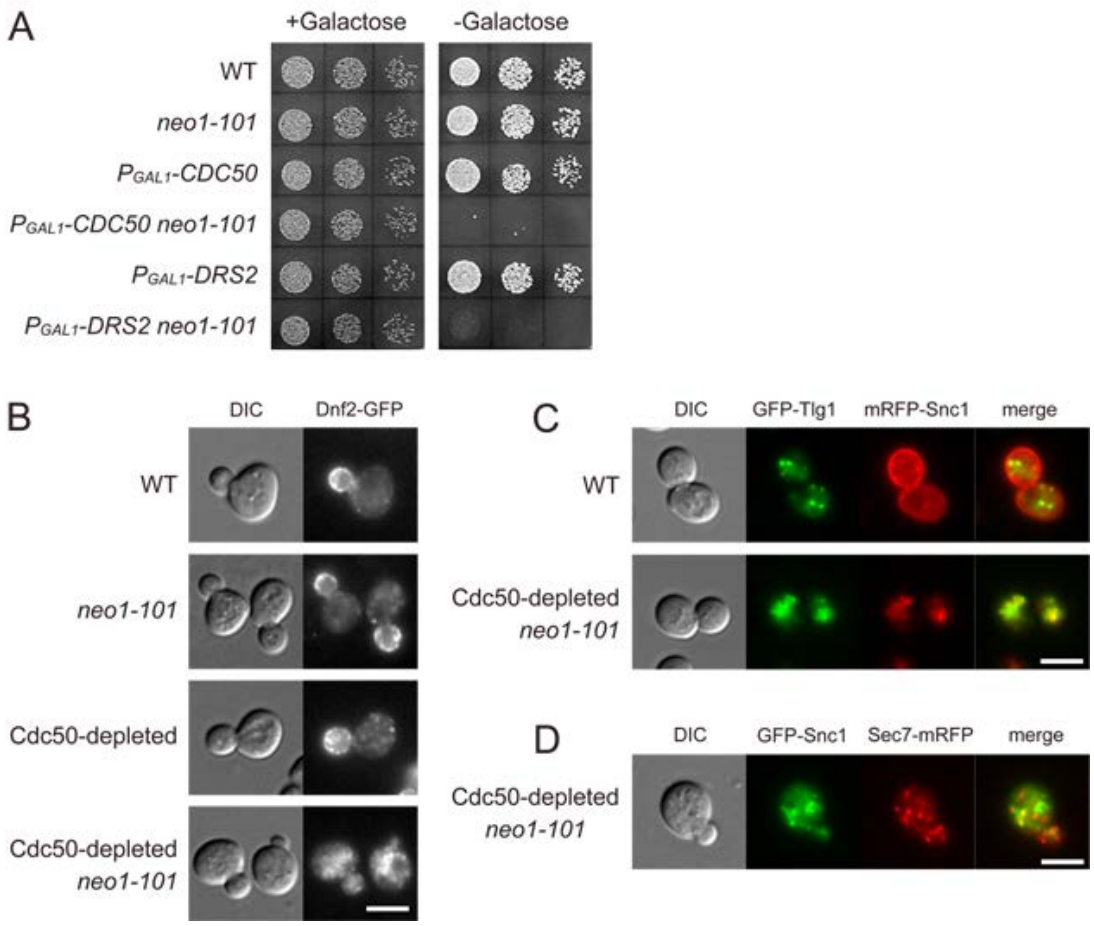

Figure 2. Cdc50p- or Drs2p-depleted *neo1-101* cells exhibit defects in growth and endocytic recycling. (A) Synthetic growth defects between *CDC50* or *DRS2* depletion and *neo1-101*. Cells were grown to early log phase in YPGA, washed, and adjusted at a concentration of 8.0×10^5 cells/ml. 4 µl drops of five-fold serial dilutions were spotted onto plates containing galactose (Cdc50p-expressed) or glucose (Cdc50p-depleted), followed by incubation at 30°C for 1 day. Strains were YKT1066 (WT, wild type), YKT1781 (*neo1-101*), YKT1782 (P_{GAL1}-*CDC50*), YKT1783 (P_{GAL1}-*CDC50 neo1-101*), YKT1629 (P_{GAL1}-*DRS2*), and YKT1784 (P_{GAL1}-*DRS2 neo1-101*). (B) Localization of Dnf2p-GFP to abnormal intracellular membranes in the Cdc50p-depleted *neo1-101* mutant. Cells were grown in YPDA medium at 30°C for 12 h, followed by microscopic examination with differential interference contrast (DIC) and GFP fluorescence (Dnf2-GFP). Strains were YKT1785 (*DNF2-GFP*) [WT], YKT1786 (*neo1-101 DNF2-GFP*), YKT1787 (P_{GAL1}-*CDC50 DNF2-GFP*, and YKT1788 (P_{GAL1}-*CDC50 neo1-101 DNF2-GFP*). (C) Colocalization of GFP-Tlg1p and mRFP-Snc1p to membrane structures in Cdc50p-depleted *neo1-101* cells. Cells harboring pRS416-GFP-TLG1 (pKT1488) were grown in SDA-U medium at 30°C for 12 h. Strains were YKT1777 (*mRFP-SNC1*) [WT] and YKT1789 (P_{GAL1}-*CDC50 neo1-101 mRFP-SNC1*). Images were merged to compare the two signal patterns. (D) The GFP-Snc1p-containing structures are independent of Sec7p-mRFP. Cells carrying pRS416-GFP-SNC1 (pKT1443) were grown in SDA-U medium at 30°C for 12 h. Strain was YKT1790 (P_{GAL1}-*CDC50 neo1-101 SEC7-mRFP*). Bars, 5 µm.

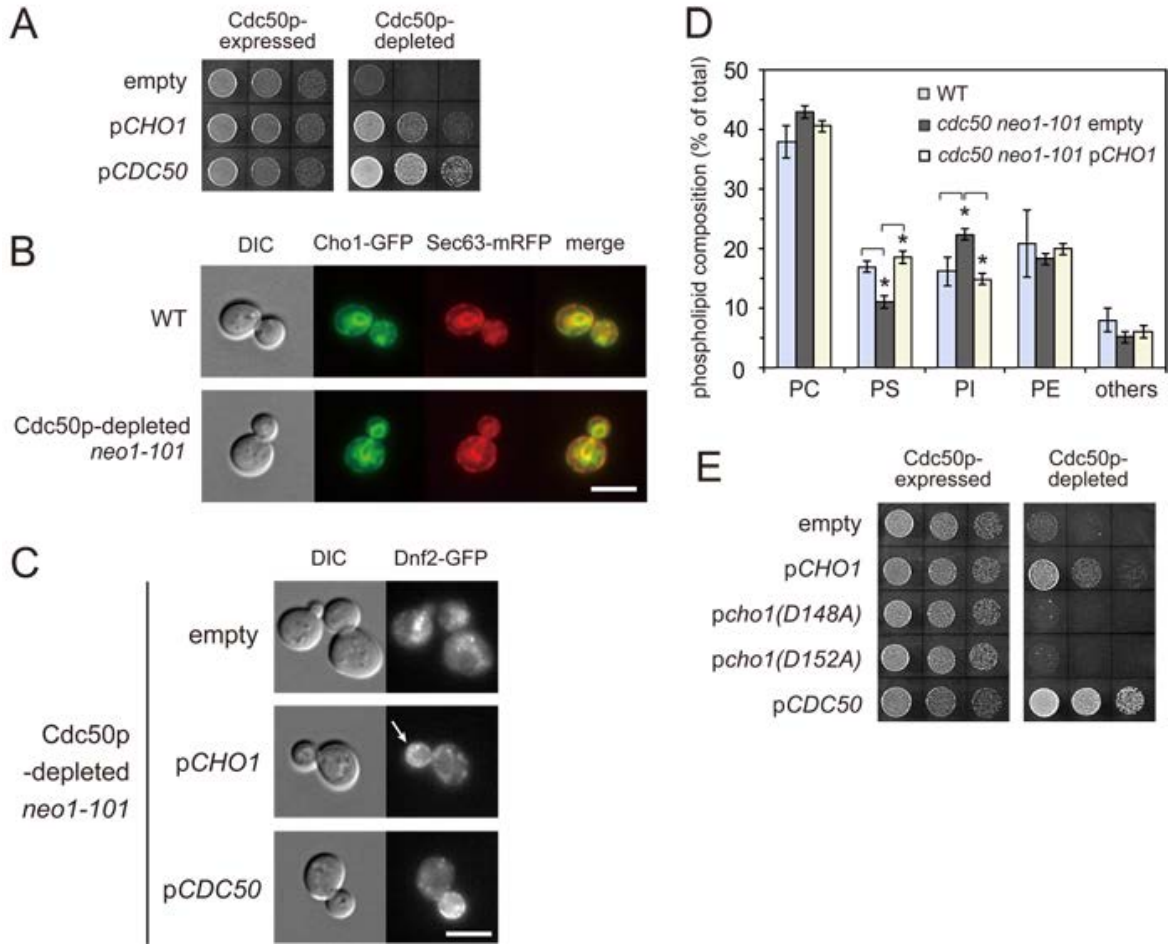

Figure 3. Overexpression of *CHO1* suppresses defects in growth and endocytic recycling of Cdc50p-depleted *neo1-101* cells. (A) Suppression of the growth defects. Cells were grown to early log phase in SGA-U medium and cell growth was examined at 30°C for 1 day as in Fig. 2A with initial cell concentration of 1.0×10^7 cells/ml. Strains were YKT1650 (P_{GAL1}-*CDC50 neo1-101*) carrying YEp24 (empty), YEp24-CHO1 (pKT1753, p*CHO1*), or YEplac195-CDC50 (pKT1263, p*CDC50*). (B) Localization of the overproduced Cho1p-GFP to the ER membrane. Cells harboring YEplac195-CHO1-GFP (pKT2112) were grown in SDA-U medium at 30°C for 12 h. Strains were YKT1871 (*SEC63-mRFP*) [WT] and YKT1872 (P_{GAL1}-*CDC50 neo1-101 SEC63-mRFP*). Bar, 5 µm. (C) Suppression of the defects in endocytic recycling of Dnf2p-GFP. Localization of Dnf2p-GFP was examined in the cells grown in SDA-U medium at 30°C for 12 h to deplete Cdc50p. Strains were YKT1788 (P_{GAL1}-*CDC50 neo1-101 DNF2-GFP*) carrying the same plasmids as in (A). Arrows indicate that Dnf2p-GFP is localized to polarized plasma membrane sites including the bud or the cytokinesis site. Bar, 5 µm. (D) PS is increased by overexpression of *CHO1*. The cells described in (A) carrying YEp24 (empty) or YEp24-CHO1 (p*CHO1*) were labeled with ^{32}P during Cdc50p depletion in SDA-U medium at 30°C for 12 h. Wild-type cells (YKT1066) carrying YEp24 were similarly cultured and ^{32}P-labeled as a control. Phospholipids were extracted, separated, and quantified as described in Materials and Methods. The data represent percentages of total phospholipids with means ± standard deviation of three independent experiments. Asterisks indicate a significant difference in the Student's

t-test (*P<0.05). PC, phosphatidylcholine; PI, phosphatidylinositol. (E) Failure of catalytically inactive *cho1* mutant genes to suppress the growth defect. Cells were grown to early log phase in SGA-U medium and cell growth was examined at 30°C for 1 day as in Fig. 2A with initial cell concentration of 2.0×10^6 cells/ml. Strains were YKT1872 (P_{GAL1}-*CDC50 neo1-101*) carrying YEplac195 (empty), YEplac195-CHO1 (pKT2111, p*CHO1*), YEplac195-cho1(D148A) [pKT2114, p*cho1(D148A)*], YEplac195-cho1(D152A) [pKT2115, p*cho1(D152A)*], or YEplac195-CDC50 (pKT1263, p*CDC50*).

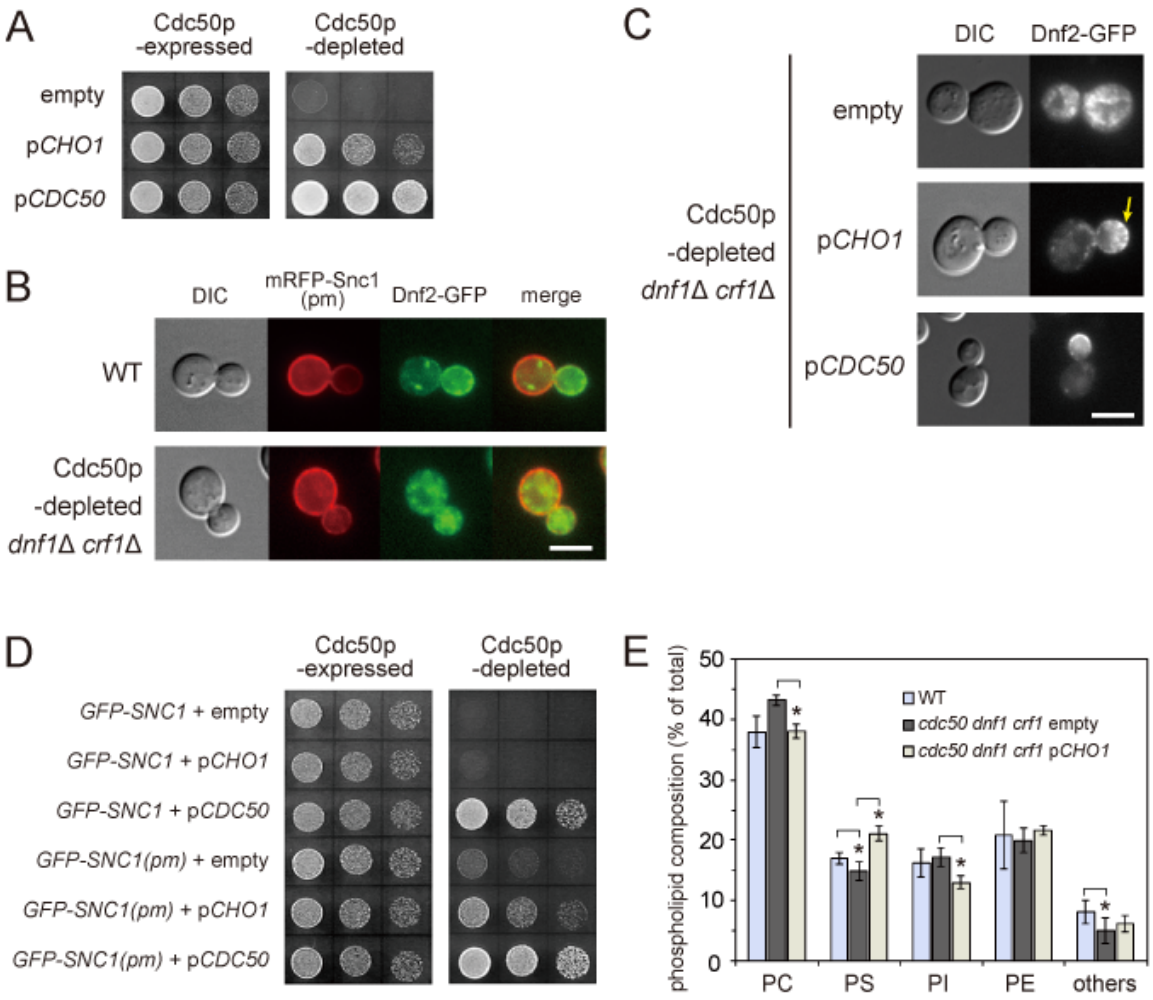

Figure 4. Overexpression of *CHO1* suppresses defects in growth and endocytic recycling of the Cdc50p-depleted *dnf1*Δ *crf1*Δ mutant. (A) Suppression of the growth defects. Cells were grown to early log phase in SGA-U medium and cell growth was examined at 25°C for 2 days as in Fig. 4A with initial cell concentration of 2.0×10^6 cells/ml. Strains were YKT1529 (P_{GAL1}-*CDC50 dnf1*Δ *crf1*Δ) carrying YEp24 (empty), YEp24-CHO1 (pKT1753, p*CHO1*), or YEplac195-CDC50 (pKT1263, p*CDC50*). (B) Localization of Dnf2p-GFP to intracellular membranes in the Cdc50p-depleted *dnf1*Δ *crf1*Δ mutant. Localization of Dnf2p-GFP and mRFP-Snc1p(pm) was examined in the cells grown in SDA-U medium at 30°C for 12 h to deplete Cdc50p. Images were merged to compare the two signal patterns. Strains were YKT1785 (*DNF2-GFP*) [WT] and YKT1791 (P_{GAL1}-*CDC50 dnf1*Δ *crf1*Δ *DNF2-GFP*) carrying pRS416-mRFP-SNC1(pm) (pKT1964). Bar, 5 μm. (C) Suppression of the defects in endocytic recycling of Dnf2p-GFP. Localization of Dnf2p-GFP was examined in the cells grown as in (B). Strains were YKT1791 (P_{GAL1}-*CDC50 dnf1*Δ *crf1*Δ *DNF2-GFP*) carrying the same plasmids as in (A). Arrows indicate that Dnf2p-GFP is localized to the polarized plasma membrane sites. Bar, 5 μm. (D) GFP tagging of Snc1p, but not of Snc1p(pm), inhibits the suppression of growth defects by *CHO1* overexpression in the Cdc50p-depleted *dnf1*Δ *crf1*Δ mutant. Cell growth was examined as in (A) at 25°C for 2 days with initial cell concentration of 8.0×10^5 cells/ml. Strains were YKT1792

(P_{GAL1}-*CDC50 dnf1*Δ *crf1*Δ *GFP-SNC1*) and YKT1793 [P_{GAL1}-*CDC50 dnf1*Δ *crf1*Δ *GFP-SNC1(pm)*] carrying the plasmids as in (A). (E) Increase of PS by overexpression of *CHO1*. Phospholipid content in the wild type and the strains described in (A) carrying YEp24 (empty) or YEp24-CHO1 (pKT1753, p*CHO1*) was analyzed as in Fig. 3D.

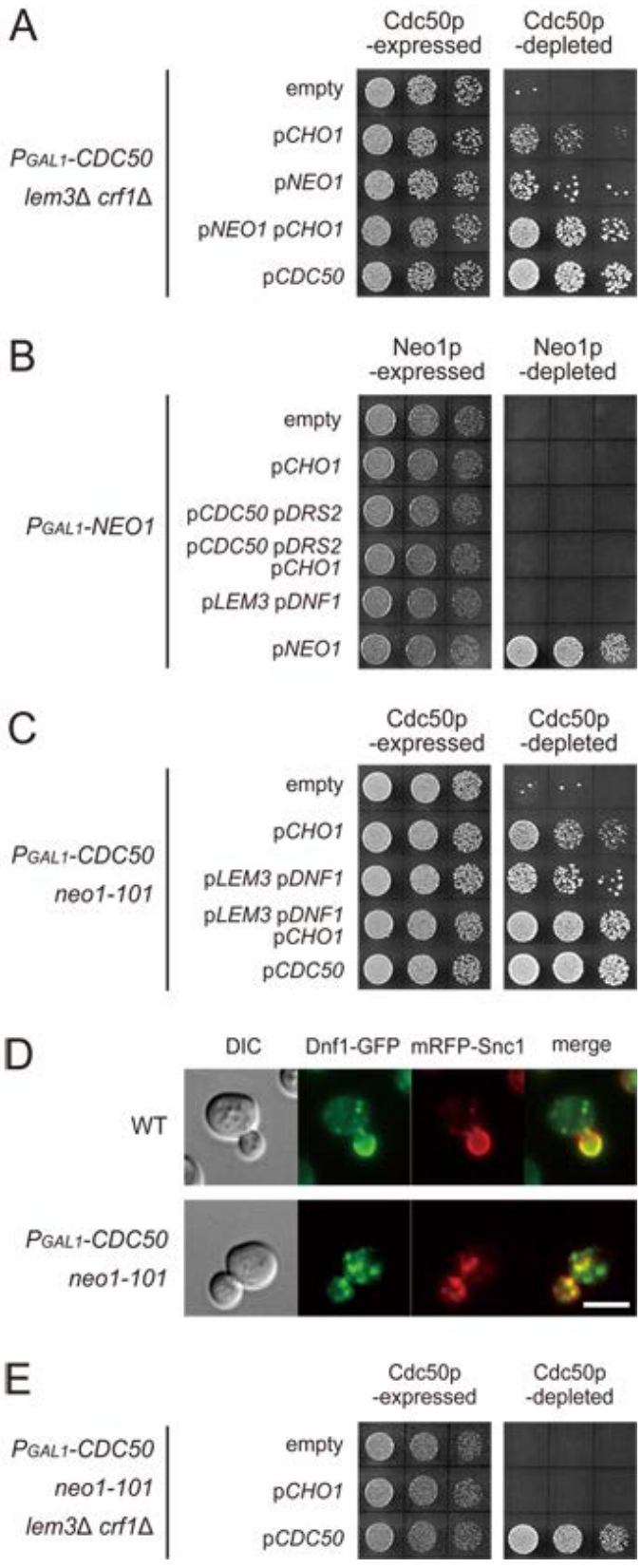
A
Cdc50p -expressed
Cdc50p -depleted
PGAL1-CDC50 lem3Δ crf1Δ
empty
pCHO1
pNEO1
pNEO1 pCHO1
pCDC50
B
Neo1p -expressed
Neo1p -depleted
PGAL1-NEO1
empty
pCHO1
pCDC50 pDRS2
pCDC50 pDRS2 pCHO1
pLEM3 pDNF1
pNEO1
C
Cdc50p -expressed
Cdc50p -depleted
PGAL1-CDC50 neo1-101
empty
pCHO1
pLEM3 pDNF1
pLEM3 pDNF1 pCHO1
pCDC50
D
DIC
Dnf1-GFP
mRFP-Snc1
merge
WT
PGAL1-CDC50 neo1-101
E
Cdc50p -expressed
Cdc50p -depleted
PGAL1-CDC50 neo1-101 lem3Δ crf1Δ
empty
pCHO1
pCDC50

Figure 5. Suppression by the *CHO1* overexpression is dependent on a remaining flippase. (A) Suppression of the growth defect in the Cdc50p-depleted *lem3*Δ *crf1*Δ mutant by *CHO1* or/and *NEO1* overexpression. Cells were grown to early log phase in SG-LU medium and cell growth was examined at 30°C for 1 day as in Fig. 2A with initial cell concentration of 4.0×10^6 cells/ml. Strains were YKT1513 (P_{GAL1}-*CDC50 lem3*Δ *crf1*Δ) carrying pRS425 and YEp24 [empty], pRS425 and YEp24-CHO1 (pKT1753) [p*CHO1*], pRS425-NEO1 (pKT1788) and YEp24 [p*NEO1*], pRS425-NEO1 and YEp24-CHO1 [p*NEO1* p*CHO1*], and pRS425 and YEplac195-CDC50 (pKT1263) [p*CDC50*]. (B) Growth defects in the Neo1p-depleted mutant are not suppressed by overexpression of either *CHO1* or other flippases. Cells were grown to early log phase in SGA-UW medium and cell growth was examined at 30°C for 1 day as in Fig. 2A with initial cell concentration of 8.0×10^5 cells/ml. Strains were YKT1660 (P_{GAL1}-*NEO1*) carrying YEplac112 and YEplac195 [empty], YEplac112-CHO1 (pKT2097) and YEplac195 [p*CHO1*], YEplac112 and YEplac195-DRS2-CDC50 (pKT1607) [p*CDC50* p*DRS2*], YEplac112-CHO1 and YEplac195-DRS2-CDC50 [p*CHO1* p*CDC50* p*DRS2*], YEplac112-LEM3 (pKT2098) and YEplac195-DNF1 (pKT1602) [p*LEM3* p*DNF1*], and YEplac112 and YEplac195-NEO1 (pKT1469) [p*NEO1*]. (C) Suppression of the growth defect in the Cdc50p-depleted *neo1-101* mutant by *CHO1* or/and *LEM3*/*DNF1* overexpression. Cells were grown to early log phase in SG-LWU medium and cell growth was examined at 30°C for 1 day as in Fig. 2A with initial cell concentration of 4.0×10^6 cells/ml. Strains were YKT1650 (P_{GAL1}-*CDC50 neo1-101*) carrying YEplac181, YEplac195, and YEplac112 [empty], YEplac181, YEplac195, and YEplac112-CHO1 (pKT2097) [p*CHO1*], YEplac181-LEM1 (pKT1340), YEplac195-DNF1 (pKT1602), and YEplac112 [p*LEM3* p*DNF1*], YEplac181-LEM1, YEplac195-DNF1, and YEplac112-CHO1 [p*LEM3* p*DNF1* p*CHO1*], and YEplac181, YEplac195, and YCplac22-CDC50 (pKT1264) [p*CDC50*]. (D) Colocalization of Dnf1p-GFP with mRFP-Snc1p in early endosomal membranes in the Cdc50p-depleted *neo1-101* mutant. Localization of Dnf1p-GFP and mRFP-Snc1p was examined in the cells grown in SDA-U medium at 30°C for 12 h to deplete Cdc50p. Strains were YKT1797 (*DNF1-GFP*) [WT] and YKT1798 (P_{GAL1}-*CDC50 neo1-101 DNF1-GFP*) carrying pRS416-mRFP-SNC1 (pKT1563). Bar, 5 μm. (E) Growth defects in the Cdc50p-depleted *neo1-101 lem3*Δ *crf1*Δ mutant are not suppressed by *CHO1* overexpression. Cells were grown to early log phase in SGA-U medium and cell growth was examined at 30°C for 1 day as in Fig. 2A with initial cell concentration of 8.0×10^5 cells/ml. Strains were YKT1796 (P_{GAL1}-*CDC50 neo1-101 lem3*Δ *crf1*Δ) carrying YEp24 [empty], YEp24-CHO1 (pKT1753) [p*CHO1*], YEplac195-CDC50 (pKT1263) [p*CDC50*].

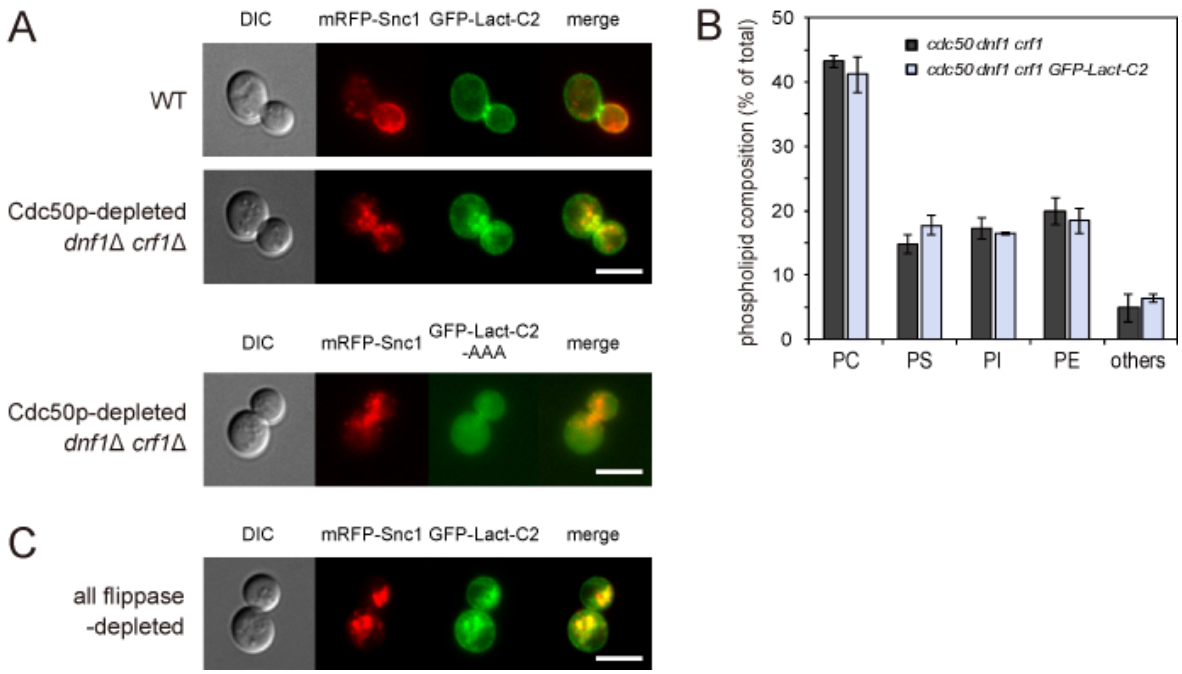

Figure 6. GFP-Lact-C2 is localized to early endosomal membranes accumulated in the flippase mutants. (A) Colocalization of GFP-Lact-C2 with mRFP-Snc1p on endosomal membranes in the Cdc50p-depleted *dnf1*Δ *crf1*Δ mutant. Localization of mRFP-Snc1p and GFP-Lact-C2 or GFP-Lact-C2-AAA was examined in the cells grown in SDA-U medium at 30°C for 12 h to deplete Cdc50p. Strains were YKT1799 (*GFP-Lact-C2*) [WT] and YKT1800 (P_{GAL1}-*CDC50 dnf1*Δ *crf1*Δ *GFP-Lact-C2*) carrying pRS416-mRFP-SNC1 (pKT1563), and YKT1801 (P_{GAL1}-*CDC50 dnf1*Δ *crf1*Δ *GFP-Lact-C2-AAA mRFP-SNC1*). (B) PS content is not affected by expression of GFP-Lact-C2 in the Cdc50p-depleted *dnf1*Δ *crf1*Δ mutant. Phospholipid content was analyzed as in Fig. 3D. Strains were YKT1529 (P_{GAL1}-*CDC50 dnf1*Δ *crf1*Δ) and YKT1800 (P_{GAL1}-*CDC50 dnf1*Δ *crf1*Δ *GFP-Lact-C2*). (C) Colocalization of GFP-Lact-C2 with mRFP-Snc1p in the Cdc50p- and Neo1p-deleted *lem3*Δ *crf1*Δ mutant. Localization of mRFP-Snc1p and GFP-Lact-C2 was examined in the cells grown in SD-L medium at 30°C for 8 h to deplete Cdc50p and Neo1p. Strain was YKT1802 (P_{GAL1}-*CDC50* P_{GAL1}-*NEO1 lem3*Δ *crf1*Δ *GFP-Lact-C2*) carrying pRS315-mRFP-SNC1 (pKT1568) [all flippase-depleted]. Bars, 5 μm.

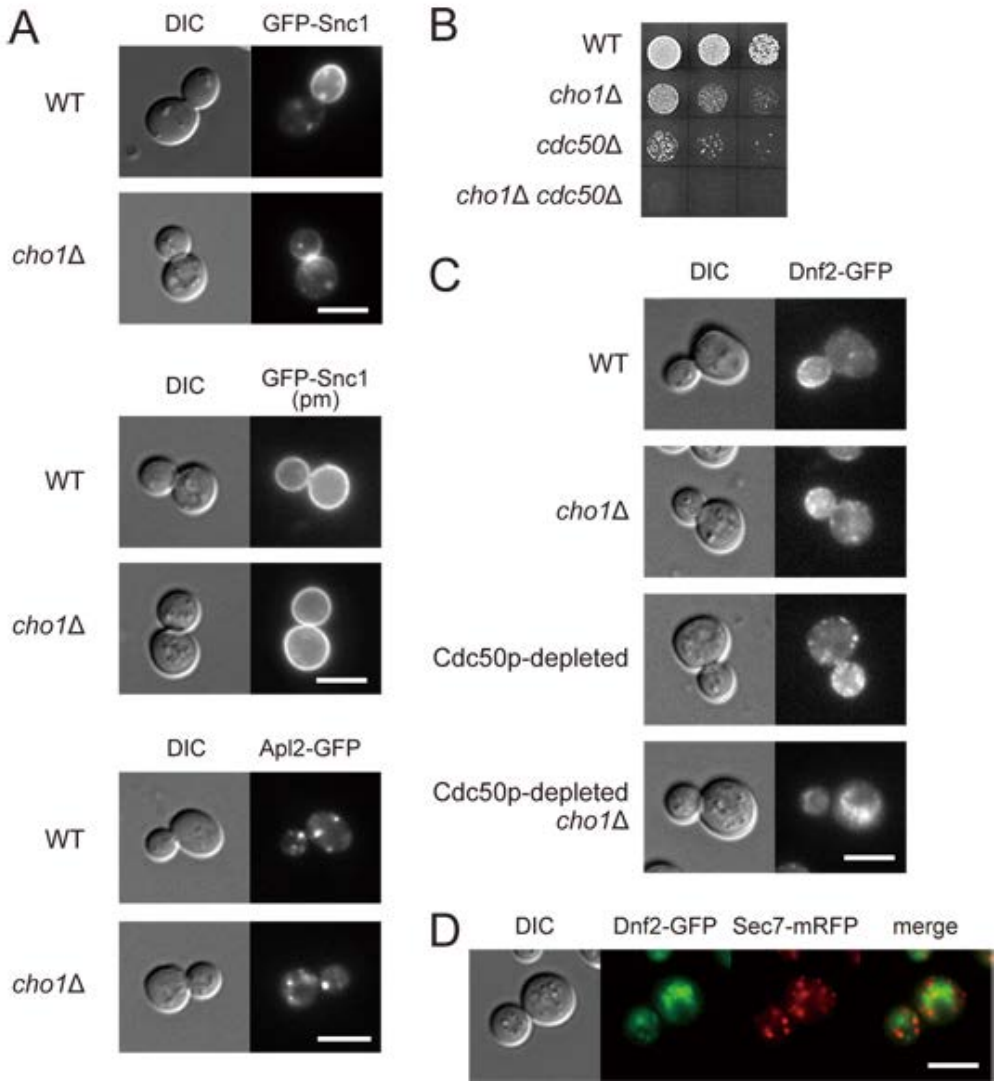

Figure 7. PS is not essential for the endocytic recycling pathway. (A) Localization of GFP-Snc1p, GFP-Snc1p(pm), and Apl2p-GFP in the *cho1*Δ mutant. Cells were grown at 30°C in SDA-U medium supplemented with 2 mM ethanolamine [for GFP-Snc1p and GFP-Snc1p(pm)] or in YPDA medium (for Apl2p-GFP), followed by microscopic examination. Strains were YKT1066 (WT) and YKT1428 (*cho1*Δ) carrying pRS416-GFP-SNC1 (pKT1443) or pRS416-GFP-SNC1(pm) (pKT1444), YKT1642 (*APL2-GFP*), and YKT1803 (*cho1*Δ *APL2-GFP*). (B) Synthetic growth defects between *cho1*Δ and *cdc50*Δ mutations. Cell growth was examined on YPDA medium as in Fig. 2A at 25°C for 2 days with initial cell concentration of 4.0×10^6 cells/ml. Strains were YKT1066 (WT), YKT1428 (*cho1*Δ), YKT1507 (*cdc50*Δ), and YKT1804 (*cho1*Δ *cdc50*Δ). (C) Localization of Dnf2p-GFP in Cdc50p-depleted *cho1*Δ cells. Localization of Dnf2p-GFP was examined in the cells grown in YPDA medium at 30°C for more than 24 h to deplete Cdc50p. Strains were YKT1805 (*DNF2-GFP*), YKT1806 (*cho1*Δ *DNF2-GFP*), YKT1787 (P_{GAL1}-*CDC50 DNF2-GFP*), and YKT1807 (P_{GAL1}-*CDC50 cho1*Δ *DNF2-GFP*). (D) Dnf2p-GFP is not colocalized with Sec7p-mRFP in the Cdc50p-depleted *cho1*Δ mutant. Cells of YKT1808 (P_{GAL1}-*CDC50 cho1*Δ *DNF2-GFP SEC7-mRFP*) were grown and observed as in C. Bars, 5 μm.

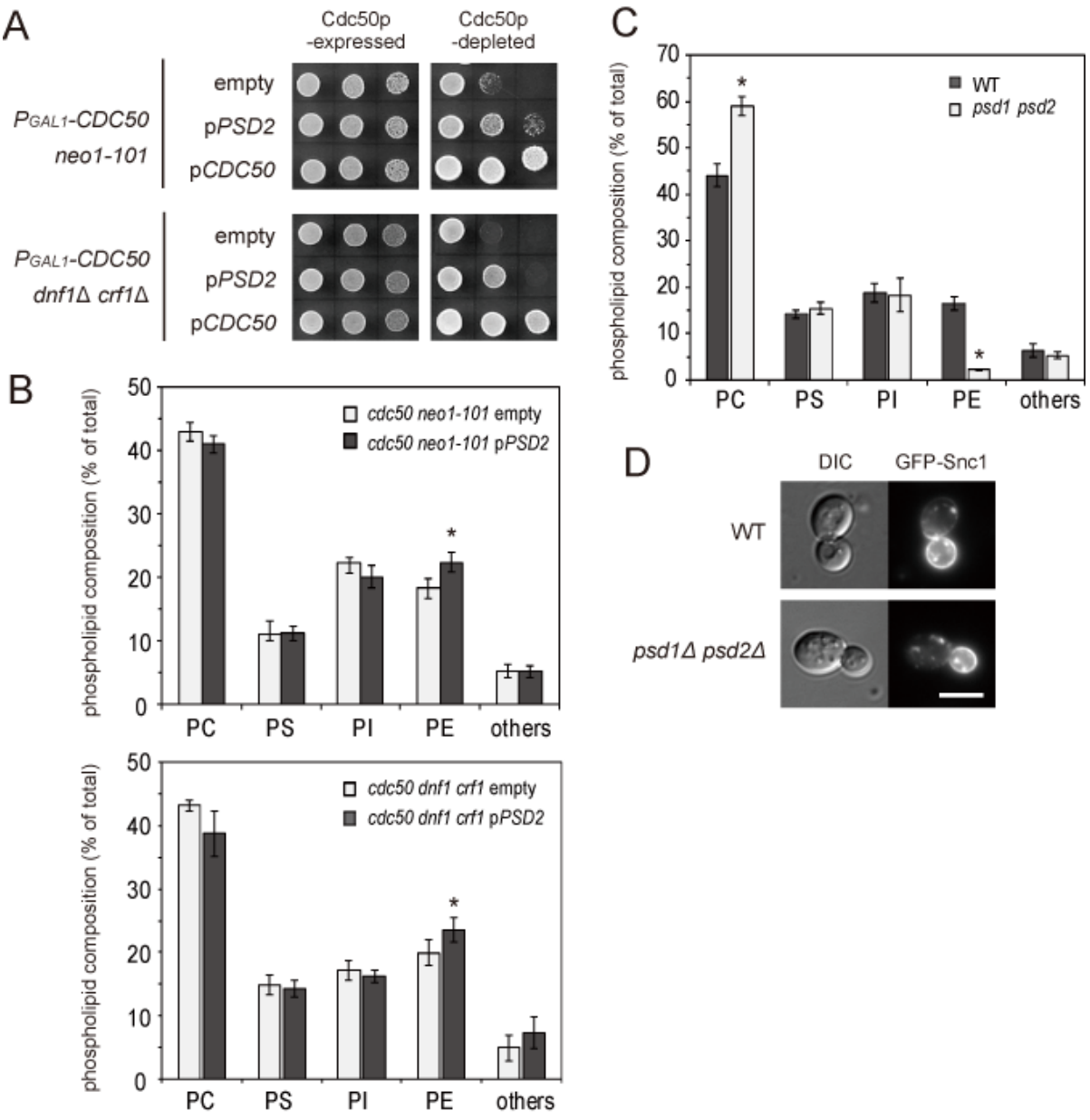

Figure 8. Increased PE also suppresses the growth defects in the Cdc50p-depleted *neo1-101* mutant and Cdc50p-depleted *dnf1*Δ *crf1*Δ mutant. (A) Suppression by overexpression of *PSD2*. Cell growth was examined on synthetic plate media (SGA-U or SDA-U) as in Fig. 2A at 25°C for 2.5 days with initial cell concentration of 2.0×10^6 cells/ml for the Cdc50p-depleted *neo1-101* mutant, and at 25°C for 2 days with initial cell concentration of 1.0×10^7 cells/ml for the Cdc50p-depleted *dnf1*Δ *crf1*Δ mutant, respectively. Strains were YKT1650 (P_{GAL1}-*CDC50 neo1-101*) and YKT1529 (P_{GAL1}-*CDC50 dnf1*Δ *crf1*Δ) carrying YEp24 (empty), YEp352-PSD2 (pKT2096, p*PSD2*) or YEplac195-CDC50 (pKT1263, p*CDC50*). (B) PE is increased by overexpression of *PSD2*. Phospholipid content was analyzed as in Fig. 3D. Strains were those carrying YEp24 (empty) and YEp352-PSD2 (p*PSD2*) in (A). (C) Decrease of PE in the *psd1*Δ *psd2*Δ mutant. Cells were grown to early log phase and ^{32}P-labeled at 30°C in SD medium supplemented with 2 mM choline. Phospholipid content was analyzed as in Fig. 3D. Increase of PC was

also observed, possibly because cells were grown with 2 mM choline. Strains were YKT1066 (WT) and YKT1809 (*psd1*Δ *psd2*Δ). (D) Localization of GFP-Snc1p in the *psd1*Δ *psd2*Δ mutant. Cells were grown at 30°C in SD medium supplemented with 2 mM choline, followed by microscopic examination. Strains were YKT1523 (*GFP-SNC1*) and YKT1810 (*psd1*Δ *psd2*Δ *GFP-SNC1*). Bar, 5 μm.

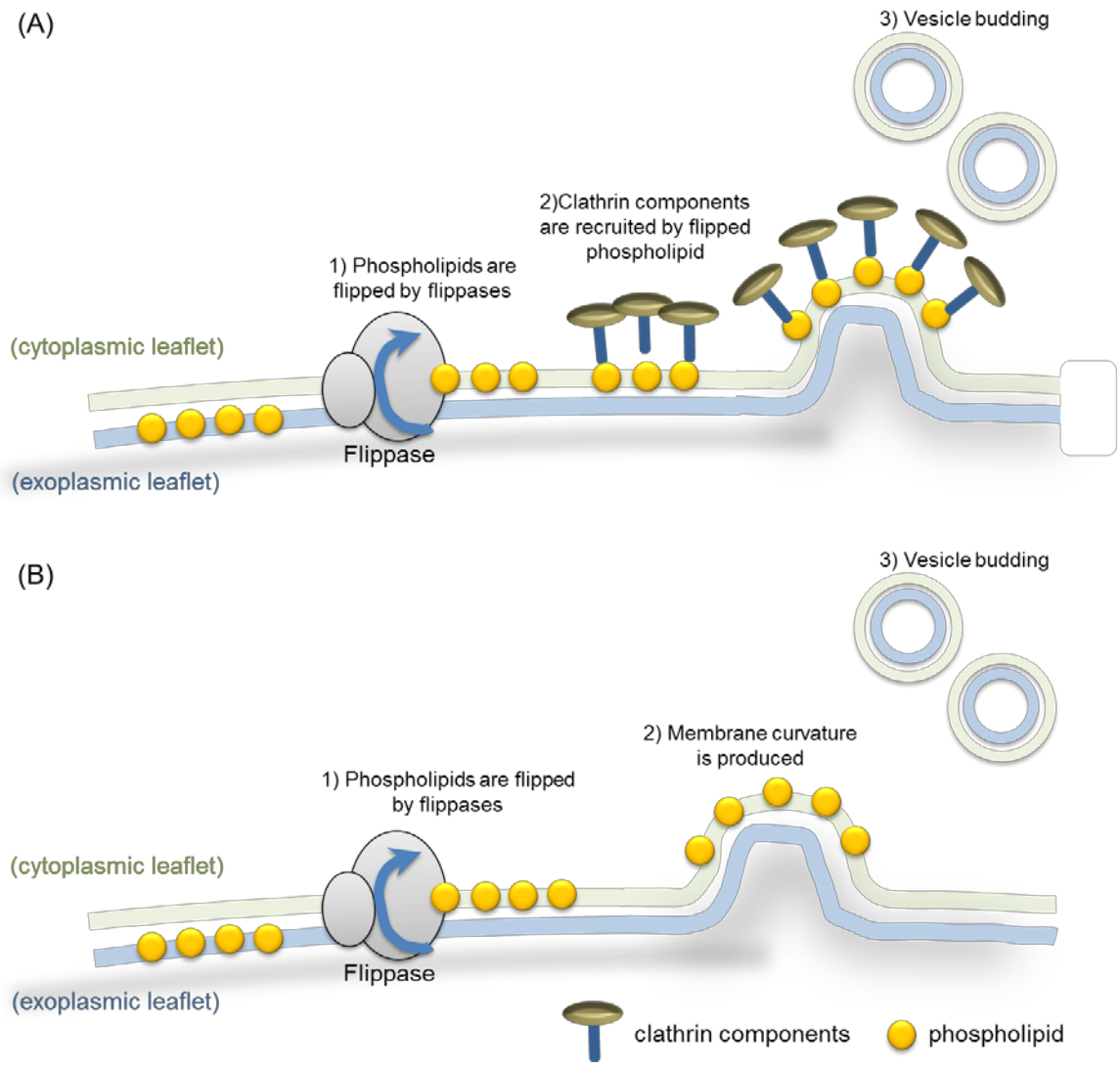

Figure 9. Two potential roles of flippases in vesicle budding. (A) Flippases produce a high concentration of substrate lipids, such as PS and PE, in the cytoplasmic leaflet. These phospholipids could recruit adaptor proteins for vesicle formation by their specific properties (e.g. a negative charge of PS). (B) Flippases flip phospholipids from the exoplasmic leaflet to the exoplasmic leaflet of lipid bilayer. An imbalance in phospholipid number induces bending in the membrane toward the cytosol, a process that is essential to vesicle budding. My results are consistent with the hypothesis (B).